Cold Spray Development for Coatings

Kumar Sridharan (University of Wisconsin, Madison)
George Young (Kairos Power, Alameda, CA)

NRC Workshop on Advanced Manufacturing
December 7th to 10th, 2020

WISCONSIN UNIVERSITY OF WISCONSIN–MADISON Argonne NATIONAL LABORATORY Kairos Power

Other Members of the Team

University of Wisconsin

Hwasung (Sung) Yeom

Kyle Quillin

Evan Willing

Mia Lenling

Tyler Dabney

Nicholas Pocquette

Kairos Power

Steven Huang

Micah Hackett

Argonne National Laboratory

Sam Sham

Mark Messner

Cold Spray Process

[Courtesy UW-Madison]

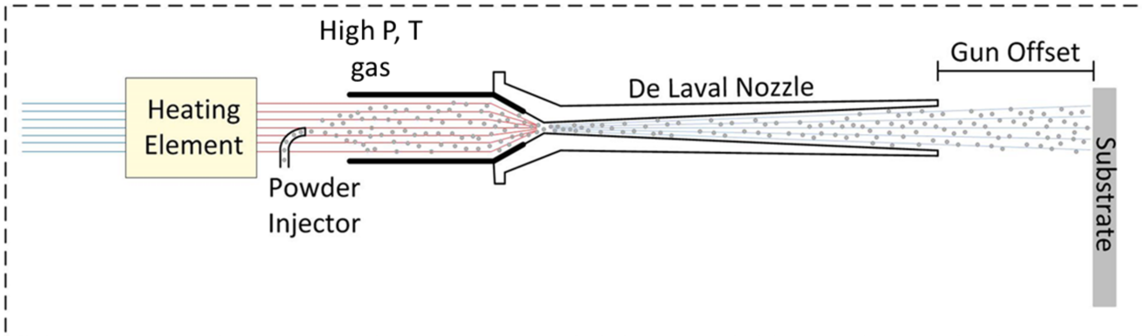

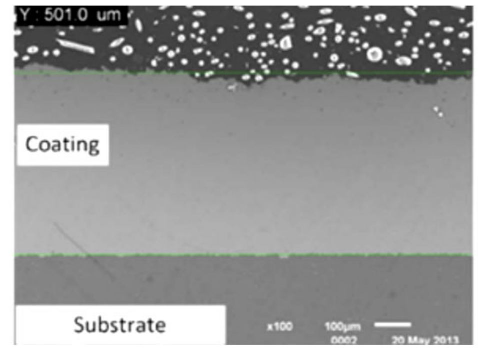

Zn cold spray coating on steel substrate

- Powder particles of the coating material propelled at supersonic velocities by a gas onto the surface of a part to form a coating or deposit
- Particle temperature is low – particles and deposition occurs in solid state
- Process performed at ambient temperature and pressure, and at very high deposition rates

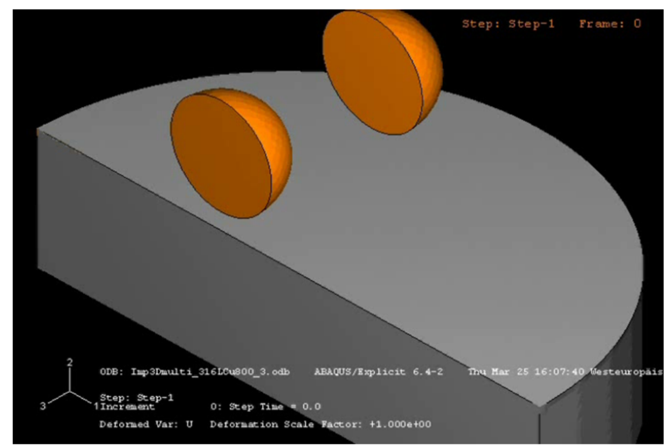

Simulation of Particle-Substrate Impact

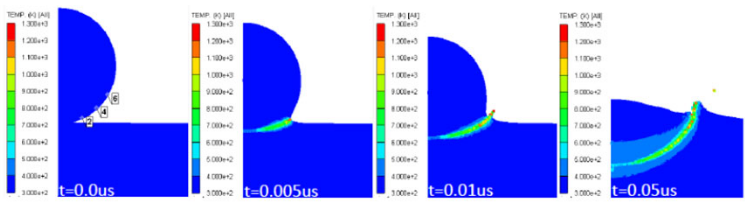

Modeling, Lane Meddaugh, Univ. Wisconsin

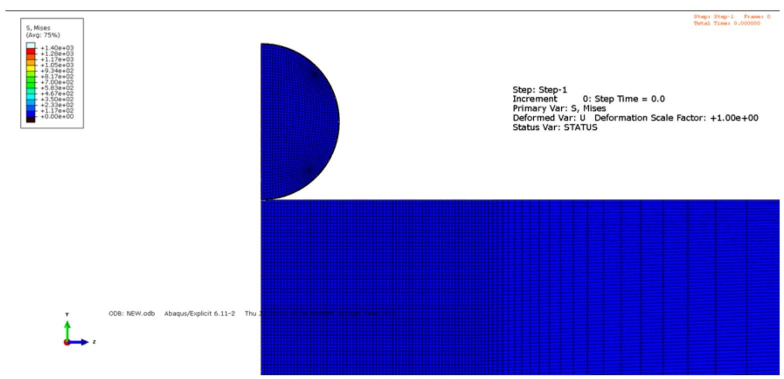

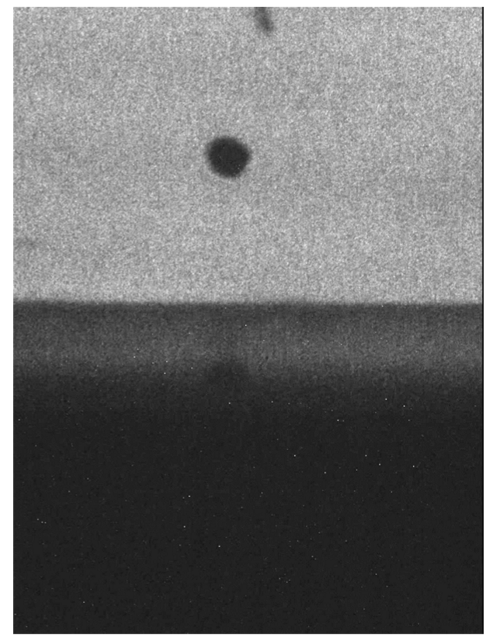

Impact of Al-particle on substrate showing jetting of oxide layer – a self-cleaning process (courtesy Dr. B. Jodoin, University of Ottawa, Canada)

Low Powder Particle Temperature

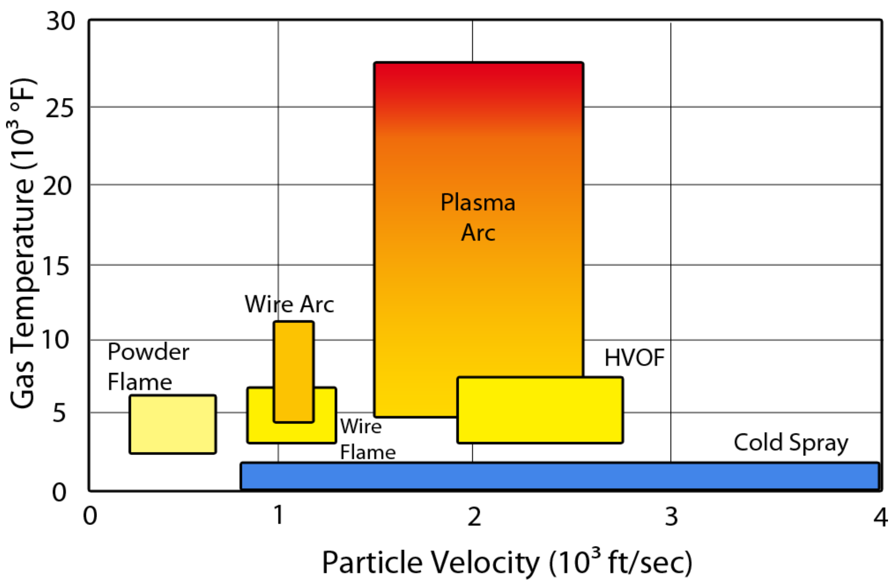

Low temperature, high particle velocity process

Low particle temperature confers several advantages:

- **Little or no oxide inclusions in the coating/deposited material**
- **Ideally suited for spraying metallic materials (e.g., Al, Cu, Ni, alloys, reactive (Ti) and refractory metals (Ta), cermets, e,g, Al/Al_2O_3, WC-Co)**
- **Recently ceramics as well, TiO_2 (Japan), Ti-Al-C (UW-Madison)**

High Deposition Efficiency

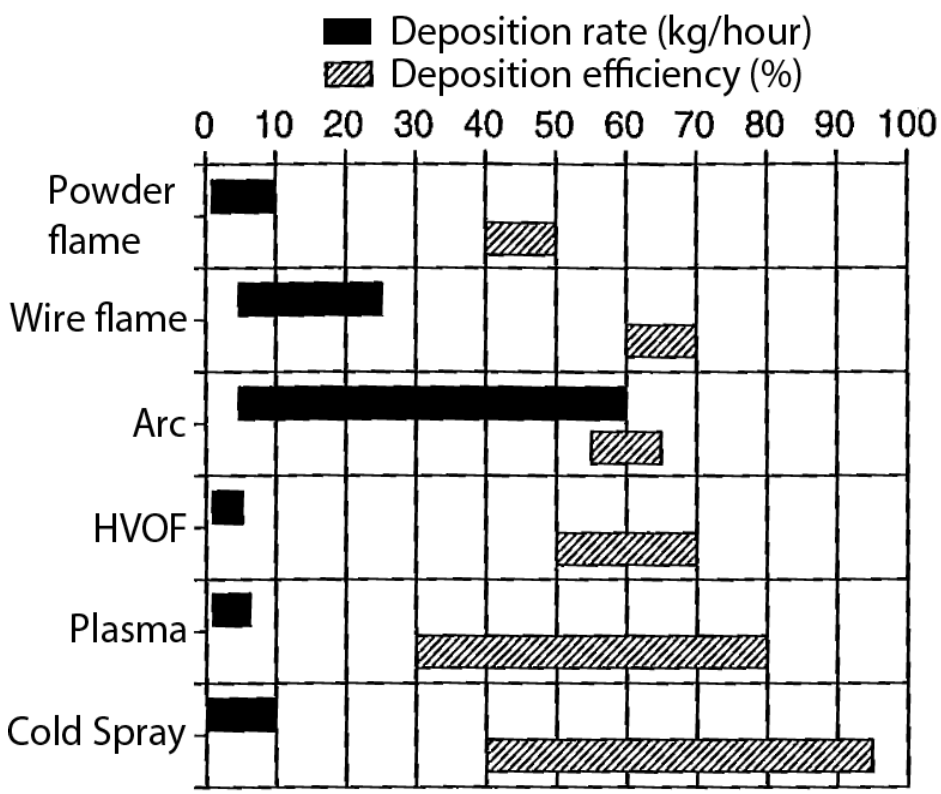

High deposition efficiencies allow for:

- **Manufacture of near-net shape products**
- **Additive manufacturing, 3D-printing**
- **Repair and dimensional restoration**

Cold Spray Laboratory at University of Wisconsin, Madison (est. 2012)

Robot for pre-programmed movement of spray gun

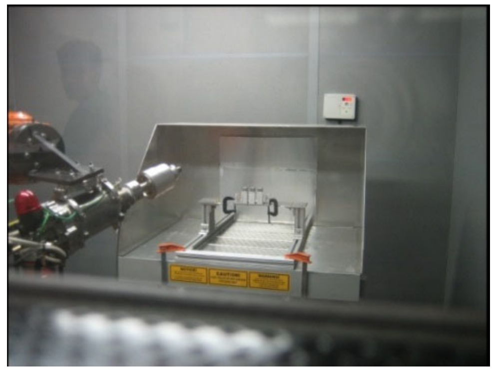

Sample stage and dust collector (below that)

Sound-proof spray booth

- **4000-34 KINETIK System, from ASB Industries/CGT-GmBH**
- **Spray booth from Noise Barriers**
- **Robot controlled (Nachi system, from Antennen)**

Nitrogen/helium gas cylinders

Robot controls (left) and spray gun control (right)

Applications of Cold Spray for Nuclear Energy Systems – ATF (with Westinghouse)

- **1300°C exposure:**

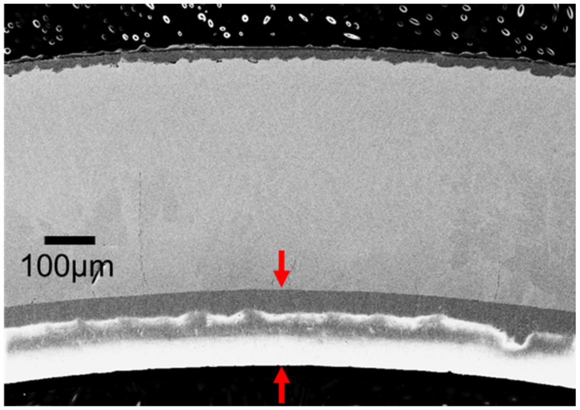

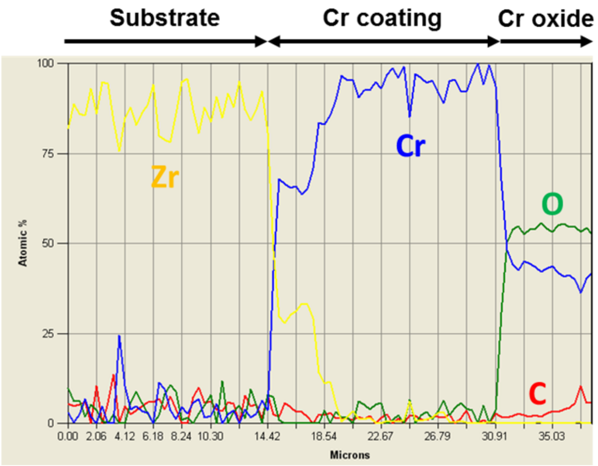

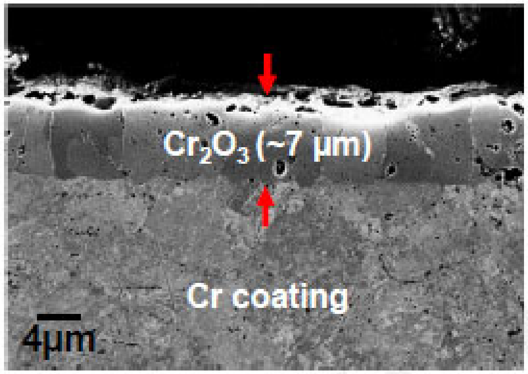

- Very thin oxide layer (~ 7µm)
- Very thin interdiffusion layer (2~3 µm)
- No interface spallation observed
- Zr-alloy side almost 200µm

Cold Spray Cr Exposure at 1300°C (with Westinghouse)

Optimized Zirlo (before test)

(a)

Optimized Zirlo coated with Cr (before test)

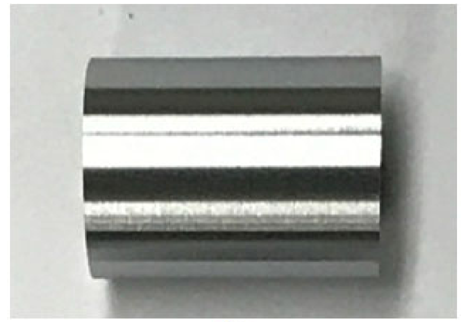

(b)

Optimized Zirlo (after test)

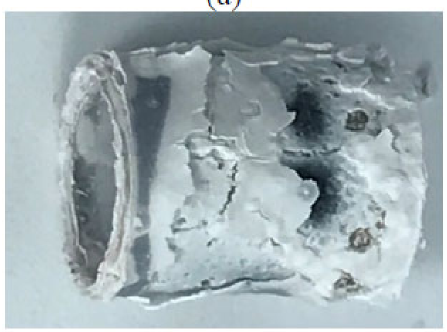

(c)

Optimized Zirlo coated with Cr (after test)

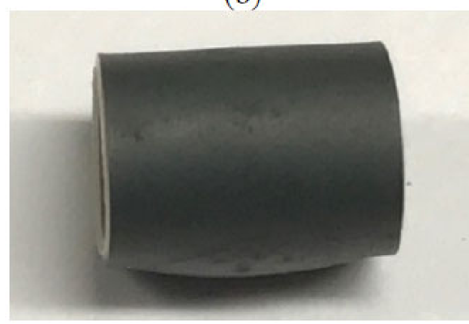

(d)

Cr coating provides good protection against oxidation

Applications of Cold Spray for Nuclear Energy Systems – ATF (with Westinghouse)

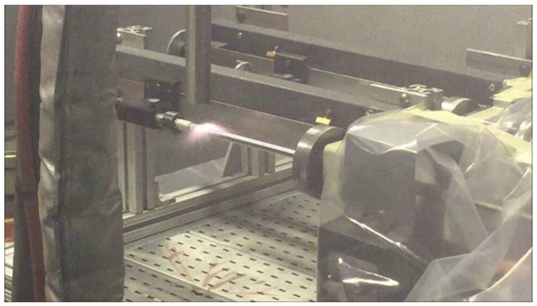

- Cr-Coating developed at UW-Madison (< 3 yrs)
- Part of WECs EnCore™ ATF program
- Joint UW-WEC patent, 2020
- Technology transfer for full-length (12') coated cladding (called lead test rods, LTR)
- In-reactor testing of LTR underway at a Utility Reactor, started in 2019

Cold Spray Coating of Zr-alloy Cladding Tubes

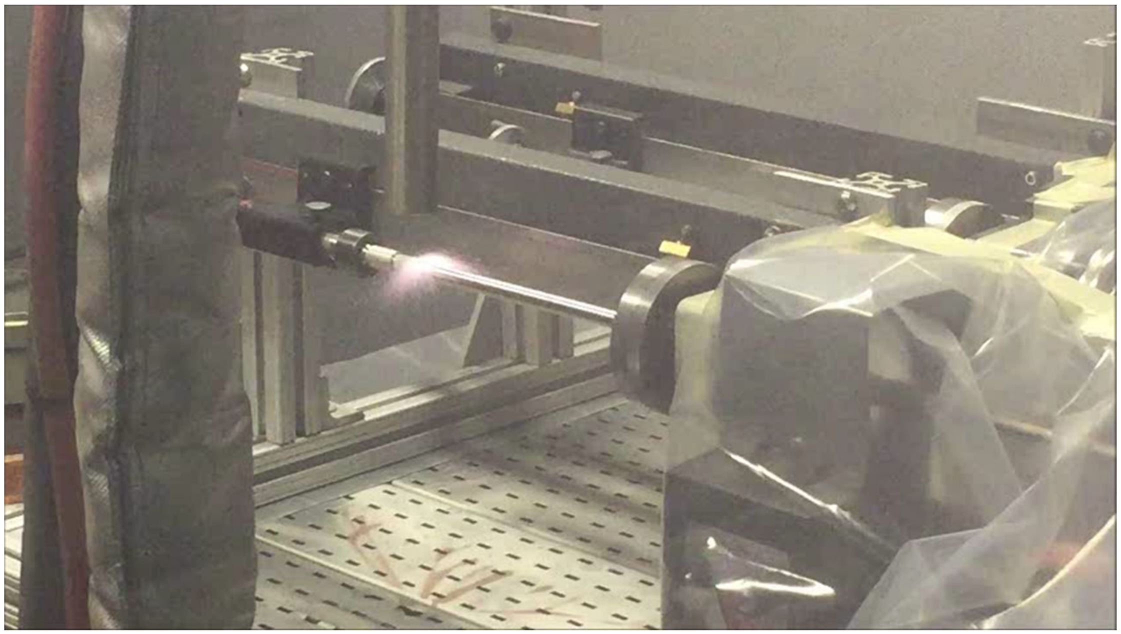

*“High Temperature Oxidation and Microstructural Evolution of Cold Spray Chromium Coatings on Zircaloy-4 in Steam Environments”, H. Yeom, B. Maier, G. Johnson, T. Dabney, M. Lenling, and K. Sridharan, **Journal of Nuclear Materials**, 526, 2019, 151737.*

*“Development of Cold Spray Chromium Coatings for Improved Accident Tolerant Zirconium-alloy Cladding”, B. Maier, H. Yeom, G. Johnson, T. Dabney, J. Walters, P. Xu, J. Romero, H. Shah, and K. Sridharan, **Journal of Nuclear Materials**, 519, 2019, p. 247.*

*“Improving Deposition Efficiency in Cold Spraying Chromium Coatings by Powder Annealing”, H. Yeom, T. Dabney, G. Johnson, B. Maier, M. Lenling, and K. Sridharan, **The International Journal of Advanced Manufacturing Technology**, 100(5), 2019, p. 1373.*

Conventional Manufacturing of ODS Steel Tubes – Slow and Expensive Process

- Milled powders -> canned and degassed at 400 ˚C -> multiple hot/ warm extrusion steps (8 -10 steps) at temperatures > 1000 ˚C and annealing.
- Low strain rate extrusion
- May lead to grain anisotropy, and anisotropy in mechanical properties
- Melting processes cannot be used as they lead to upward stratification of oxide nanoparticles (heterogeneous dispersion)

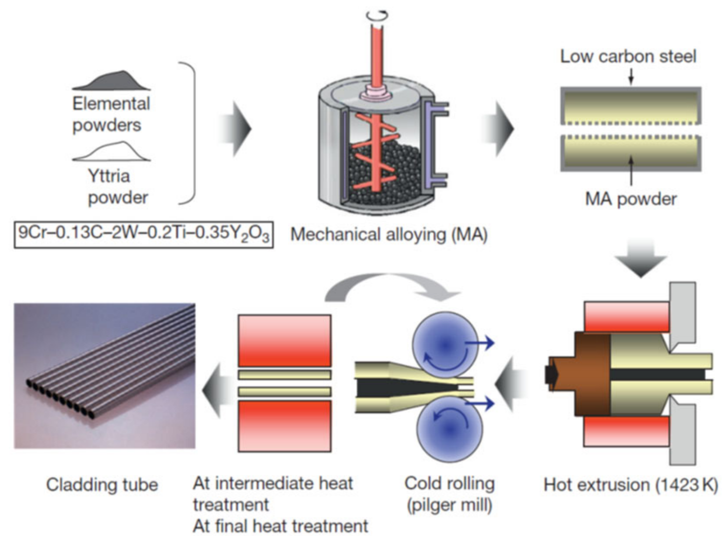

Conventional fabrication of ODS steel tubes requires mechanical alloying and multiple extrusion steps [G. Odette et al, Ann. Rev. Mater Res., 2008]

Particle Size Distributions for Ni and W Powders

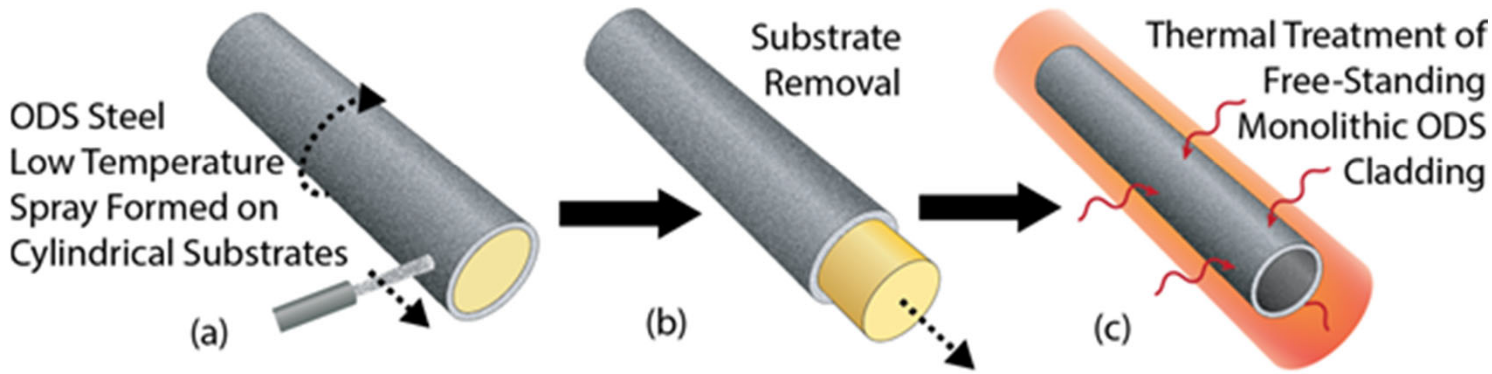

Potential Benefits:

- **Eliminates multiple extrusion steps**
- **Eliminate ball milling step**
- **Faster and cheaper manufacturing process**

Free-Standing ODS Cladding Tube Manufactured Using Gas Atomized Powder using Cold Spray

ODS Steel Flat

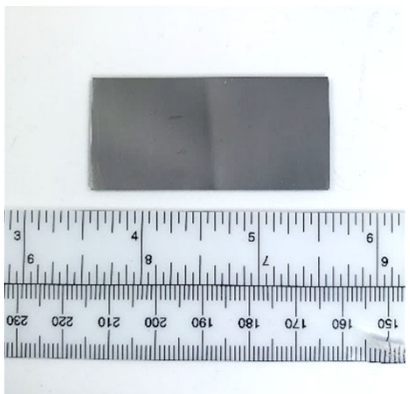

Cross-section of ODS cladding tube

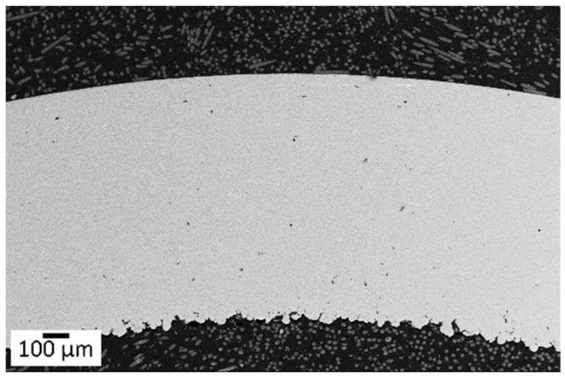

Free-standing ODS cladding tube

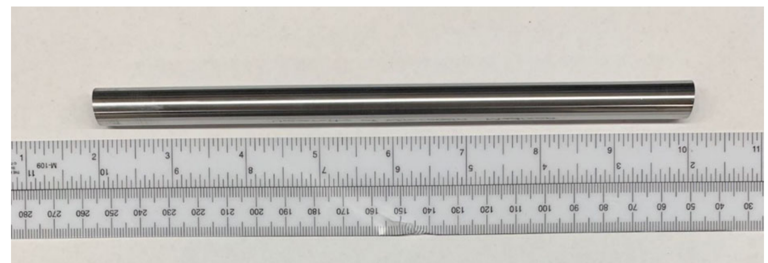

Length: 204 mm (8”) cladding tube
O.D.: 11.5 mm
Wall Thickness: ~ 1 mm

“Improving Deposition Efficiency in Cold Spraying Chromium Coatings by Powder Annealing”, H. Yeom, T. Dabney, G. Johnson, B. Maier, M. Lenling, and K. Sridharan, ***The International Journal of Advanced Manufacturing Technology****, 100(5), 2019, p. 1373.*

“A Novel Approach for Manufacturing Oxide Dispersion Strengthened (ODS) Steel Cladding Tubes using Cold Spray Technology”, B. Maier, M.Lenling, H. Yeom, G. Johnson, S. Maloy, and Kumar Sridharan, ***Nuclear Engineering and Technology****, 51, 4, 2019, p. 1069.*

Cold Spray for Mitigation and Repair of Stress Stainless Steel Canisters for Used Fuel Dry Cask Storage

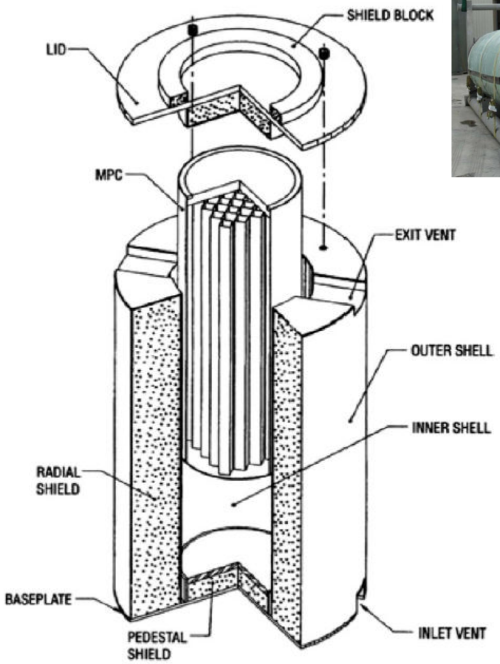

[Nuclear Waste Technical Review Board, 2010]

CISCC in 304L stainless steel

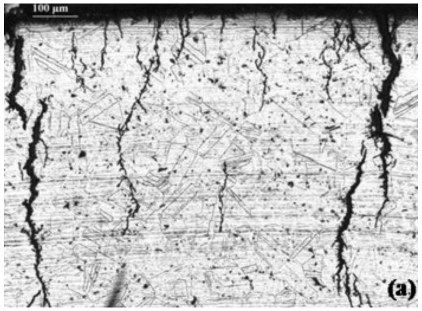

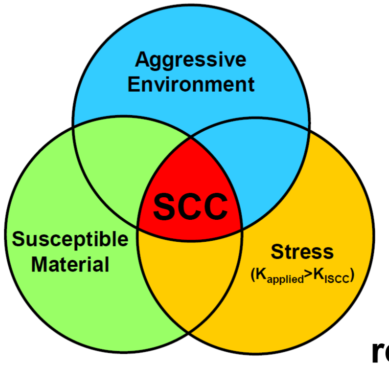

Weld residual stress

Traditional GTAW process

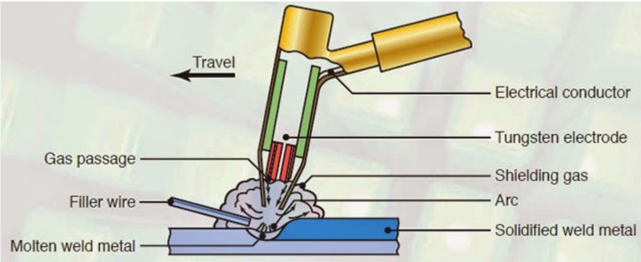

Cold Spray for Mitigation and Repair of Stress Stainless Steel Canisters for Used Fuel Dry Cask Storage

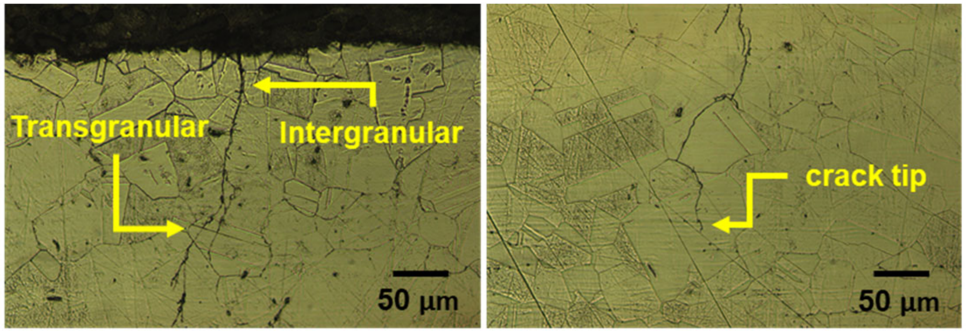

CISCC produced by partnering lab PNNL using the $MgCl_2$ Boiling Test Apparatus

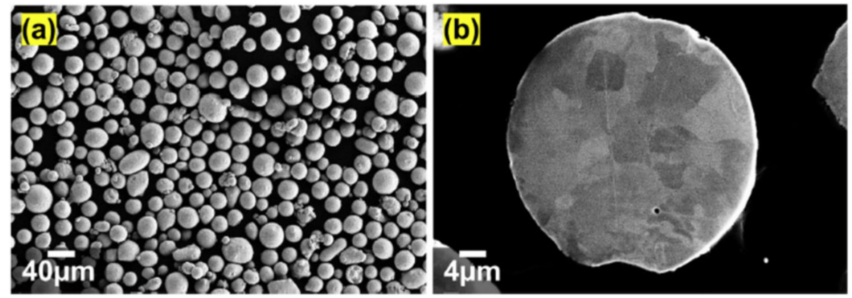

Starting Powder

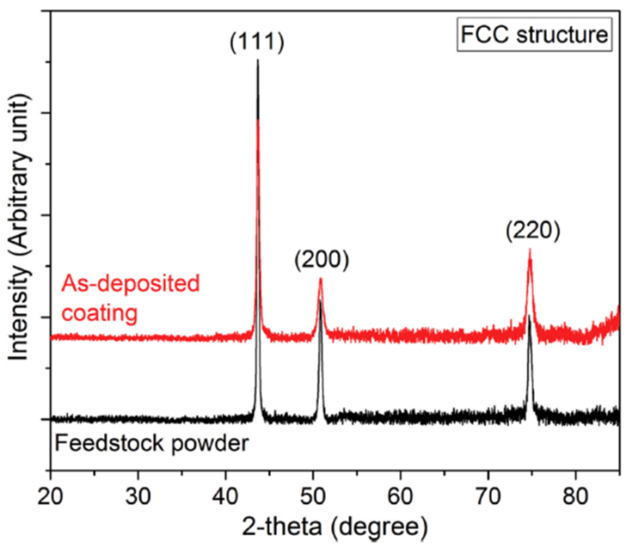

X-ray Diffraction Patter of the Powder and the coating

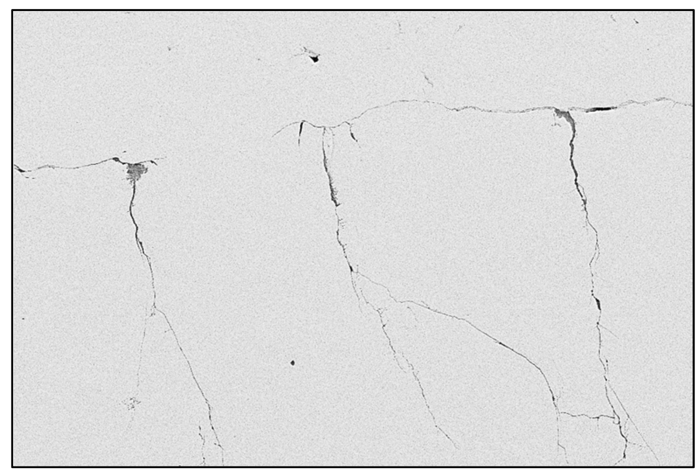

Dense cold spray coating on CISCC

Cold Spray for Mitigation and Repair of Stress Stainless Steel Canisters for Used Fuel Dry Cask Storage

Propellant gas condition	Surface residual stress (MPa)		
	Parallel to spray direction	45° direction	Perpendicular to spray direction
700 °C N_2 gas	−207 (−30.0 psi)	−216 (−31.3 psi)	−252 (−36.5 psi)
550 °C N_2/He (50/50)	−246 (−35.7 psi)	−314 (−45.6 psi)	−350 (−50.8 psi)
550 °C N_2/He (25/75)	−350 (−50.8 psi)	−396 (−57.5 psi)	−452 (−65.5 psi)

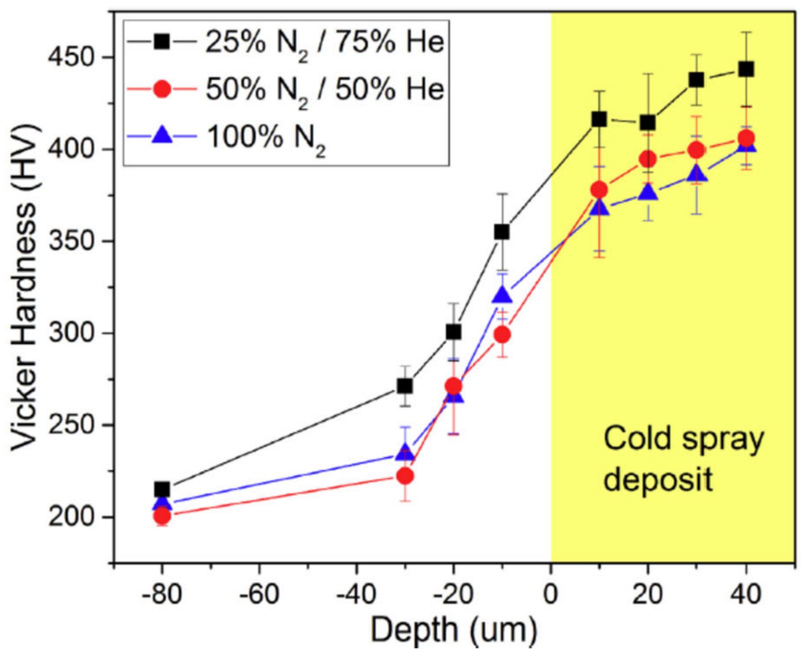

Microhardness the cold spray coating and substrate

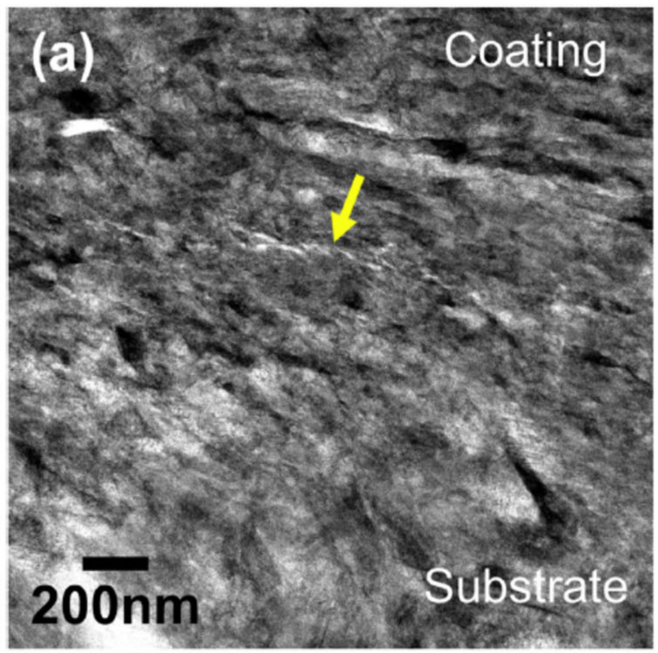

TEM image of cold spray coating and substrate

*"Cold Spray Deposition of 304L Stainless Steel to Mitigate Chloride-Induced Stress Corrosion Cracking in Canisters for Used Nuclear Fuel Storage", H. Yeom, T. Dabney, N. Pocquette, K. Ross, F. E. Pfefferkorn, and K. Sridharan, **Journal of Nuclear Materials**, vol. 538, 2020,152254.*

Corrosion and Tritium Diffusion Barrier Coatings for Fluoride Salt-Cooled High Temperature Reactor (FHR) – Preliminary Studies

Materials Corrosion in Molten Fluoride Salt is an Important Consideration for FHR

- **The less negative the free energy of formation of a metal-fluoride, is the more corrosion-resistant the metal is likely to be in molten fluoride salts**

- **W, Ni, Mo satisfy this requirement**

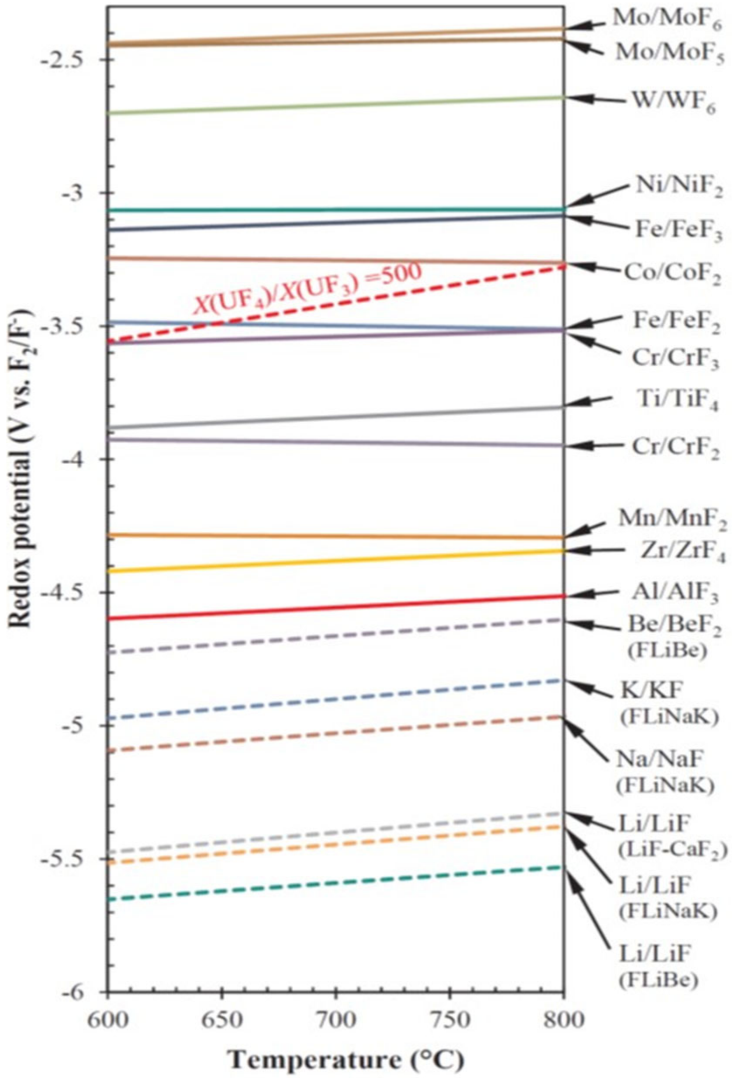

316 Stainless Steel after Corrosion Tests in FLiBe after 1000, 2000, & 3000hrs/700°C

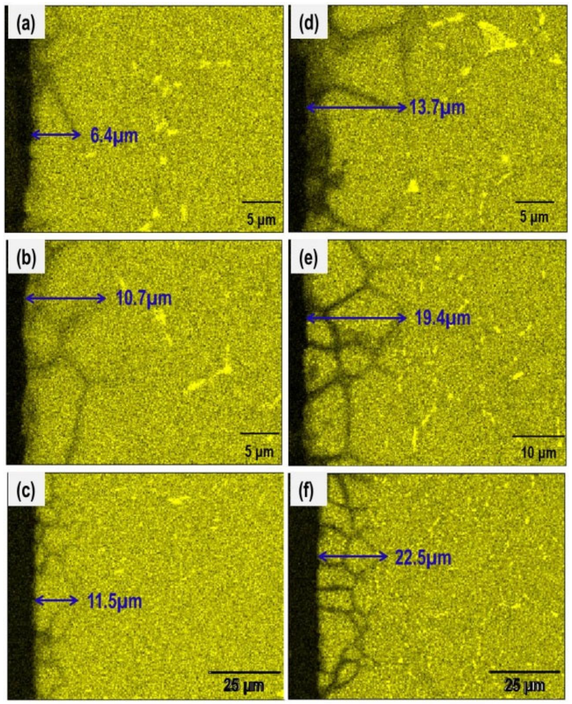

1000h

2000h

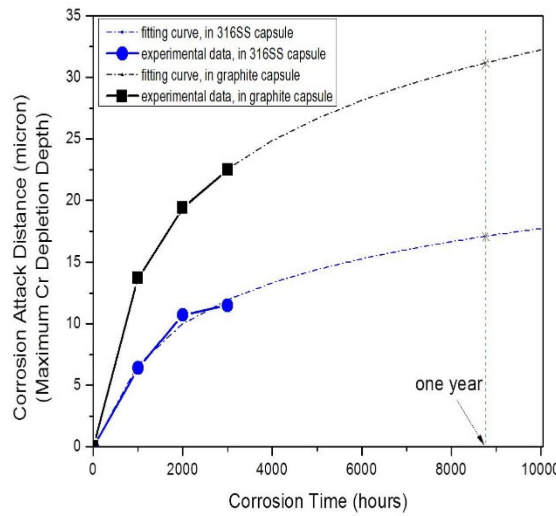

TEM of Corrosion layer

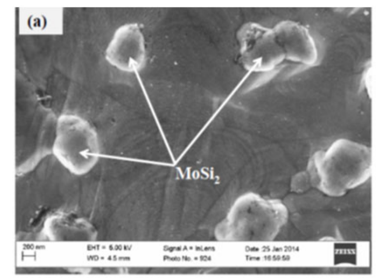

In 316 stainless steel
3000 hours

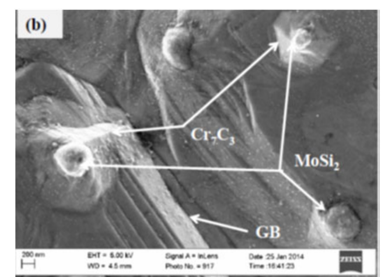

In graphite
3000 hours

In 316 st. steel (left) and in graphite capsules (right)

- **Grain boundary attack dominates**
- **Graphite accelerates corrosion but also forms carbides**

"*Corrosion of 316 Stainless Steel in High Temperature Molten Li_2BeF_4 (FLiBe) Salt", G. Zheng, B. Kelleher, G. Cao, M. Anderson, K. Sridharan, T. R. Allen, **Journal of Nuclear Materials**, vol. 416, 2015, p. 143.*

Tritium Diffusion Through Materials

- Tritium will be generated due to neutron reaction with FliBe (coolant for FHR)
- KP-FHR's Tritium Management Strategy is to assure that all environmental releases are monitored and comply with licensed pathways and limits
- The formation of tritium fluoride will be mitigated through reactions with beryllium metal to avoid corrosion
- Kairos Power is developing several methods by which tritium transport will be controlled, e.g. low permeability cladding

$$ {}^{6}_{3}LiF + n \rightarrow He + TF $$

$$ {}^{7}_{3}LiF + n \rightarrow He + TF + n' $$

$$ BeF_2 + n \rightarrow {}^{4}_{2}He + {}^{6}_{2}He + 2F^- $$

$$ {}^{6}_{2}He \rightarrow {}^{6}_{3}Li + e^+ + \overline{\nu}_e \ (t_{\frac{1}{2}} = 0.8\ s) $$

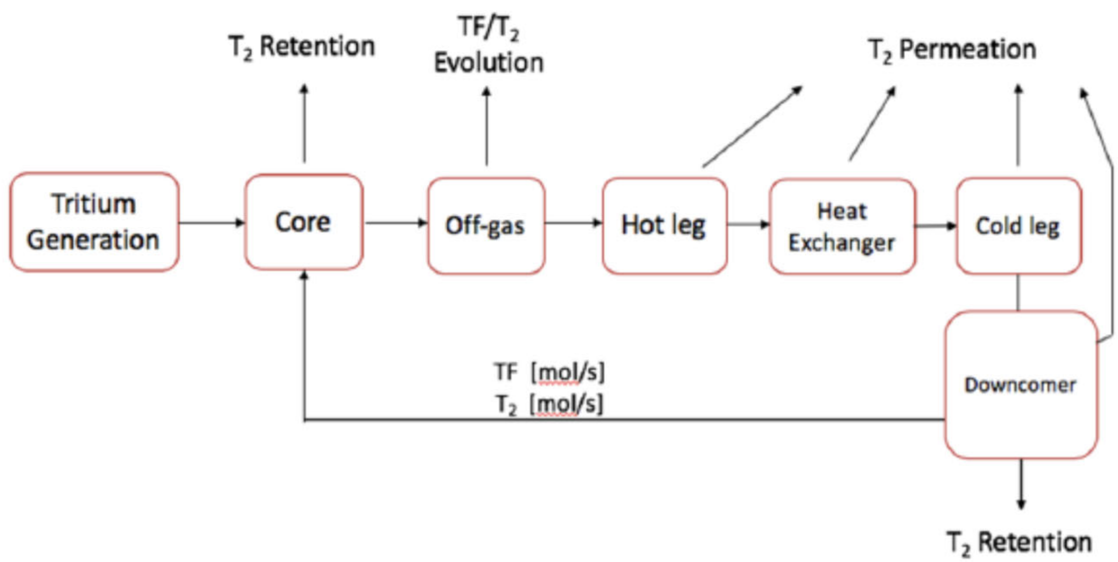

Tritium Diffusion Through Materials

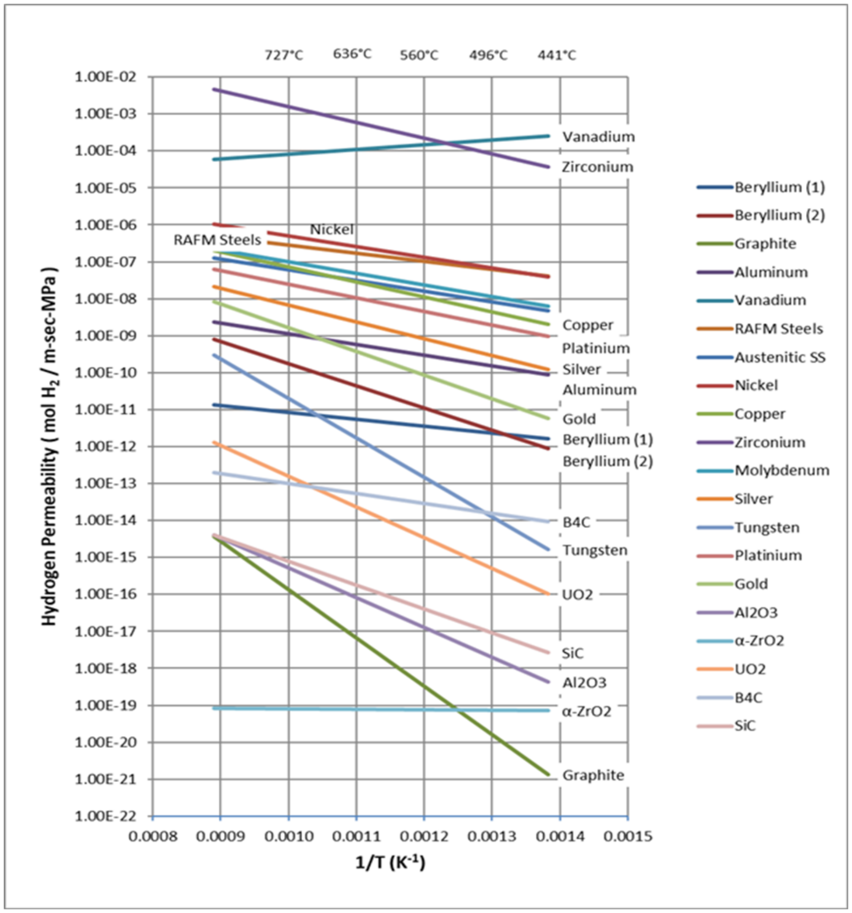

Table 1. Recommended diffusivity and solubility relationships for protium in various metals and classes of alloys in the absence of trapping.

Alloy	Diffusivity $D = D_o \exp(-E_D/RT)$ D_o $\left(\frac{m^2}{s}\right)$	E_D $\left(\frac{kJ}{mol}\right)$	Solubility, Φ/D $K = K_o \exp(-\Delta H_s/RT)$ K_o $\left(\frac{mol\ H_2}{m^3 \cdot \sqrt{MPa}}\right)$	ΔH_s $\left(\frac{kJ}{mol}\right)$	Ref.
Beryllium	3×10^{-11}	18.3	18.9 * 5.9×10^{6} *	16.8 * 96.6 *	[73] [43] [78]
Graphite	9×10^{-5}	270	19	-19.2	[43]
Aluminum	2×10^{-8}	16	46	39.7	[220] [150]
Vanadium	3×10^{-8} †	4.3 †	138	-29	[127] [197]
RAFM steels ‡	1×10^{-7}	13.2	436	28.6	
Austenitic stainless steel	2×10^{-7}	49.3	266	6.9	[95]
Nickel	7×10^{-7}	39.5	564	15.8	[153]
Copper	1×10^{-6}	38.5	792	38.9	[154]
Zirconium	8×10^{-7}	45.3	3.4×10^{7}	35.8	[143] [221]
Molybdenum	4×10^{-8}	22.3	3300	37.4	[198]
Silver	9×10^{-7}	30.1	258	56.7	[199] [200]
Tungsten	6×10^{-4}	103.1	1490	100.8	[53]
Platinum	6×10^{-7}	24.7	207	46.0	[202]
Gold	5.6×10^{-8}	23.6	77900 §	99.4 §	[205]

* per the text, the solubility of hydrogen in beryllium is very low and there is not good agreement between the few studies of the material
† data for isotopes other than protium does not scale as the square root of mass
‡ values are averaged over the data presented in Figure 12 and Figure 13
§ estimated using the permeability from Ref. [203] and the quoted diffusivity.

From [Causey]

Tritium Diffusion Through Materials

- W coatings are desirable for both corrosion resistance and low tritium permeability
- Currently evaluating several coatings (carbide, oxide, metallic) and methods (thermal spray, cold spray, explosion bonding, etc.)
- Note Kairos / ANL (Messner & Sham) GAIN to develop ASME rules for corrosion resistant cladding

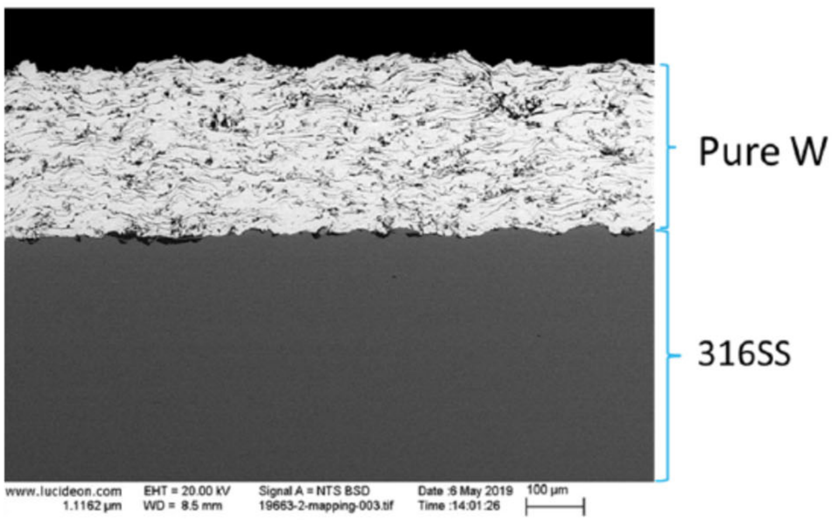

Thermal Sprayed W

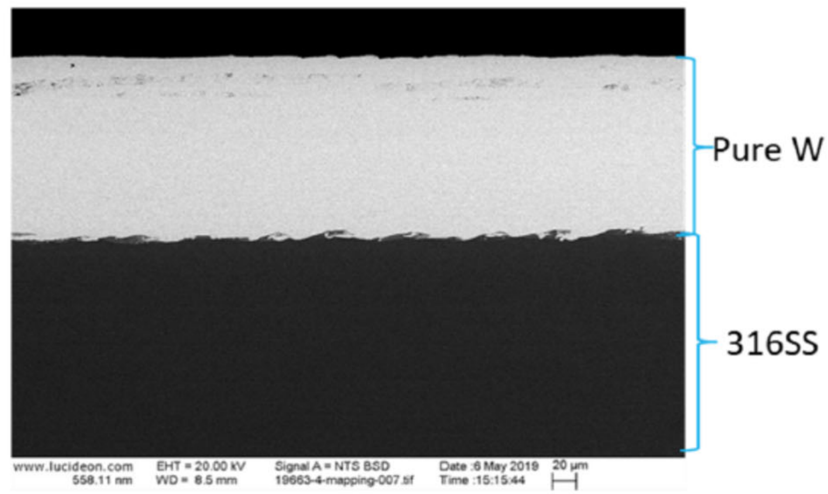

Explosion Bonded W

Work performed by Kairos Power

Investigating Ni-W Composite for a Combination of Corrosion and Tritium Diffusion

Powder Type	Sample ID	Substrate Dimension (Quantity)
Pure Ni	20190625n01/n02	1.25” × 6” (2)
Mixture of Ni and W (~16 wt.% Ni)	20190711n01/n02	1.25” × 6” (2)
Mixture of Ni and W (~10 wt.% Ni)	20190719n01/n02	1.25” × 6” (2)
Mixture of Ni and W (~5 wt.% Ni)	20190725n01/n02	1.25” × 6” (2)
Ni-coated W	20190731n01/n02	1.25” × 6” (2)
Mixture of Ni and W (~2 wt.% Ni)	20191029n01/n02	1.25” × 6” (2)
Mixture of Ni and W (~1 wt.% Ni)	20191031n01/n02	1.25” × 6” (2)

- Two 1.25” × 6” samples of each coating type produced for testing at Kairos
- One 1.25” × 2” sample produced for cross-section characterization at UW
- Atlantic Equipment Engineers provided the gas atomized 99.9% Ni-powder
- Tekna provided the 99.7% W-powder
- Global Tungsten and Powder provided 6% Ni-coated powder
- SS316H substrate was provided by McMaster-Carr.

Particle Size Distributions for Ni and W Powders

- Both powders sieved to -25µm before spraying
- Average Ni particle size ~20µm
- Average W particle size ~12µm
- Ni-coated W powder sizes range from 5-32µm

As-received Ni powder

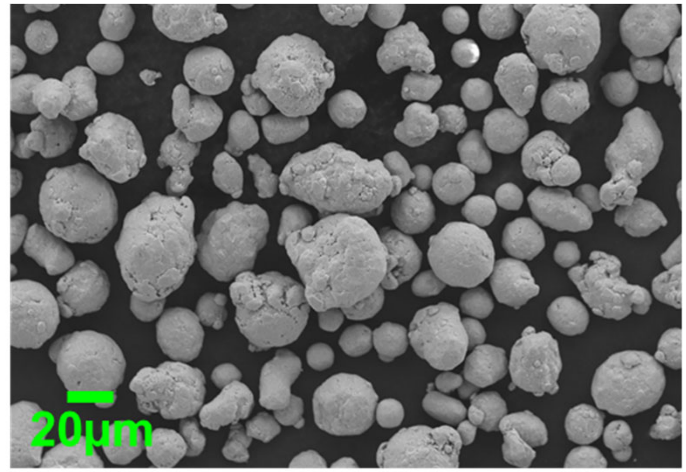

As-received W powder

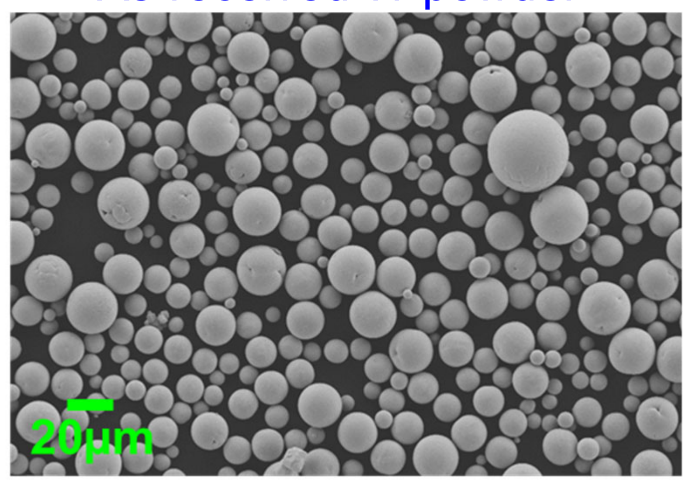

Microstructure of Ni and W Powder

- **Both powders showed equiaxed and micron-scale grained microstructure**
- **Fine Ni-oxide particulates were detected in Ni matrix as an impurity – generally shown in gas atomized powders**

Ni powder (cross-section)

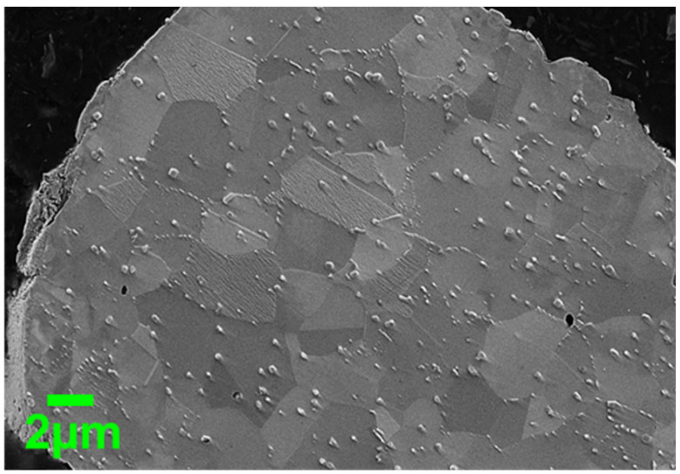

W powder (cross-section)

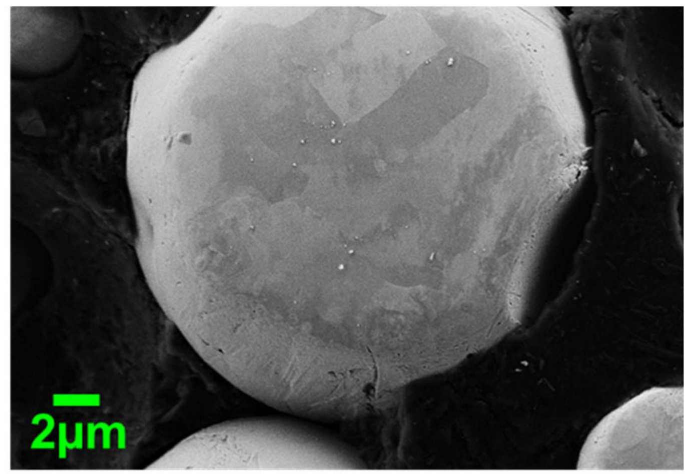

EDS analysis

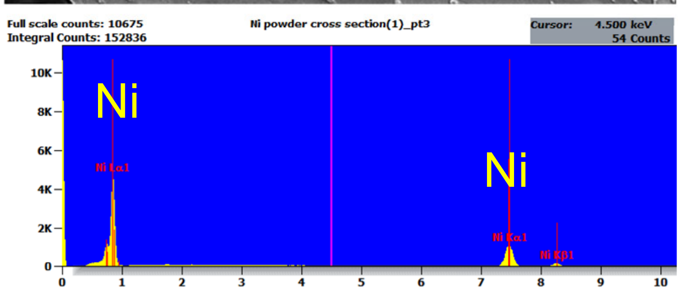

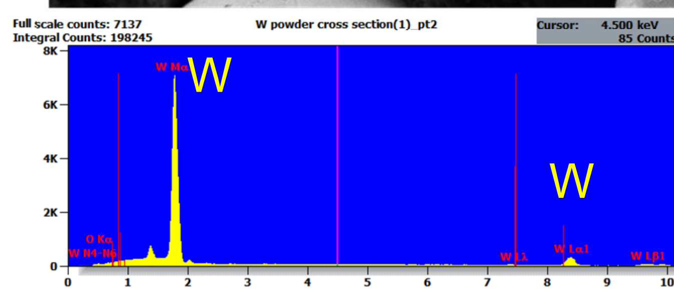

Structure of Ni-Coated W Powder

Ni coating on W particle (deposited possibly by chemical vapor deposition (CVD), is very thin, less than 500nm

Cross section images of as-received Ni-coated W powder

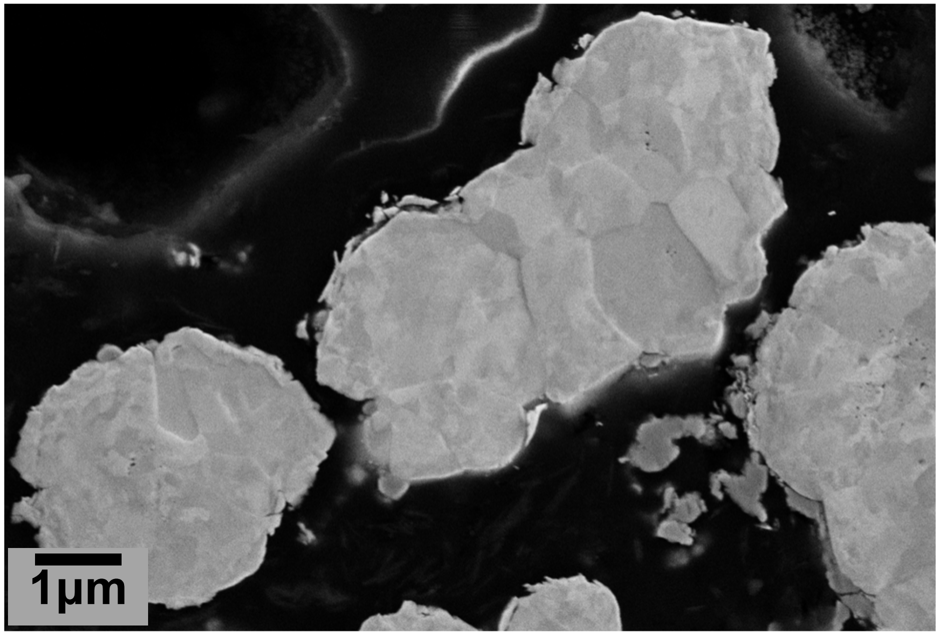

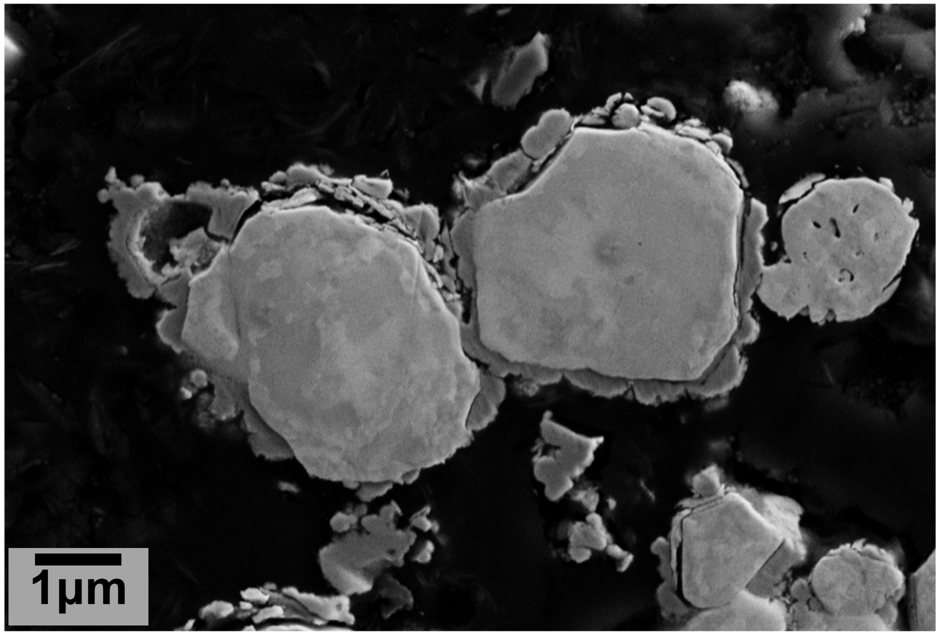

Individual particles are less than 5μm.

Pure Ni Coating

As-deposited pure Ni coating

Polished to remove surface roughness

The pure Ni coating was polished to remove surface roughness and provide a more uniform coating for testing at Kairos

Polished coating ~400-420μm thick

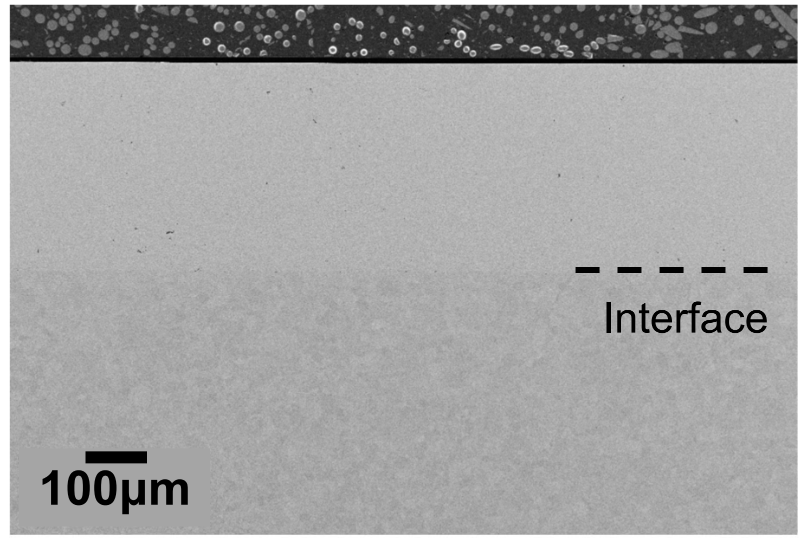

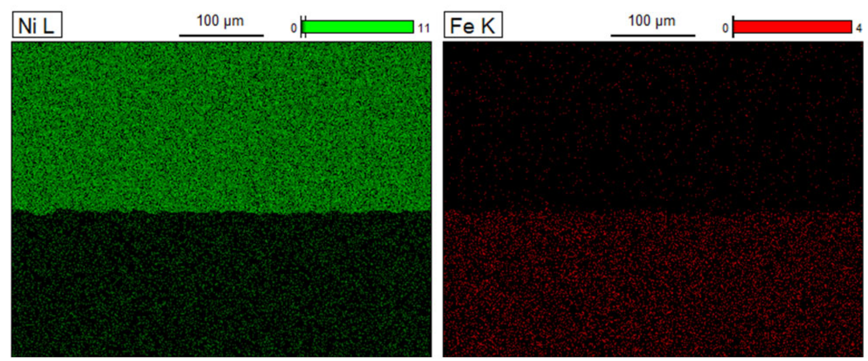

Pure W Coating

As-deposited coating ~7-20µm thick

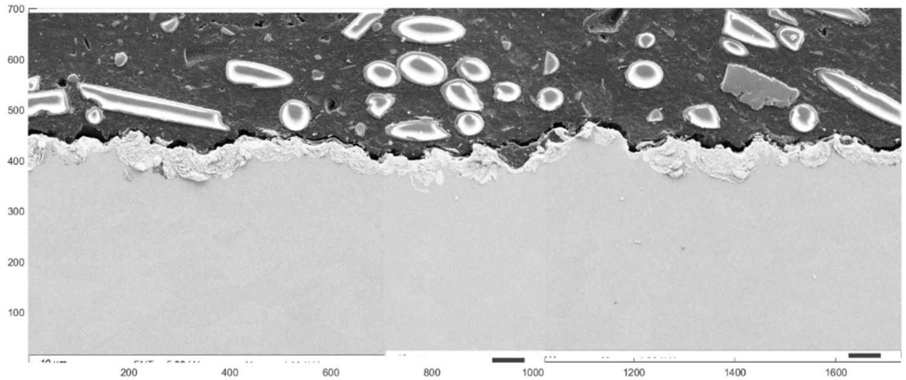

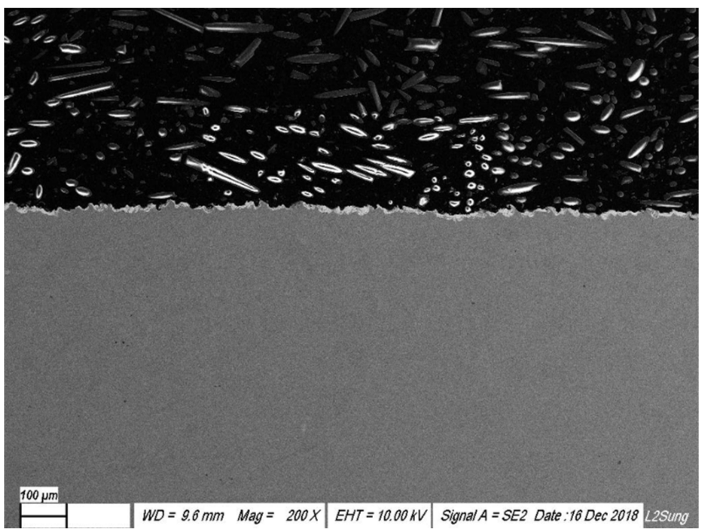

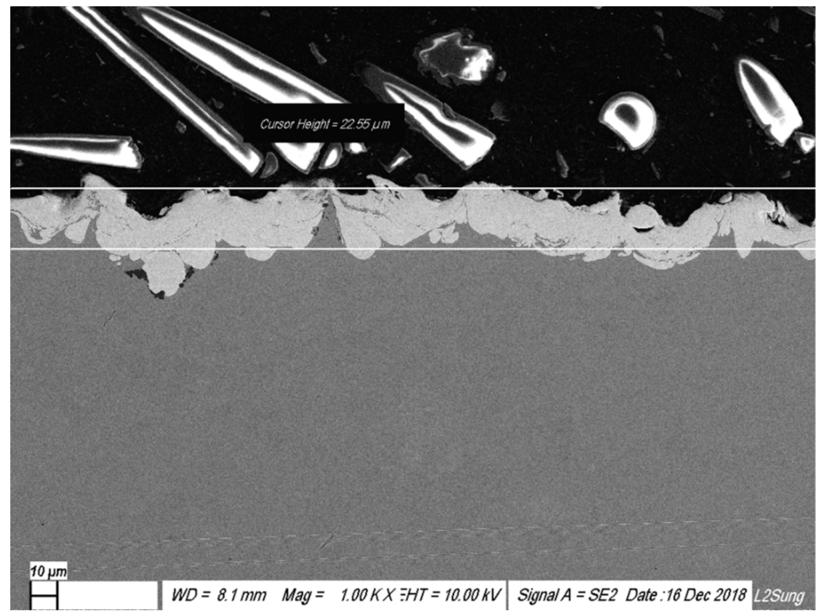

Ni-W Mixture Coatings

Pure Ni and W powders were blended together in three compositions:

- 16 wt.% Ni
- 10 wt.% Ni
- 5 wt.% Ni

As-deposited 5 wt. % Ni coating

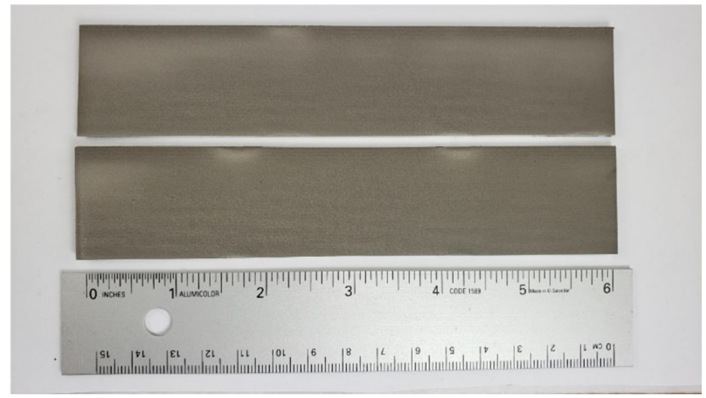

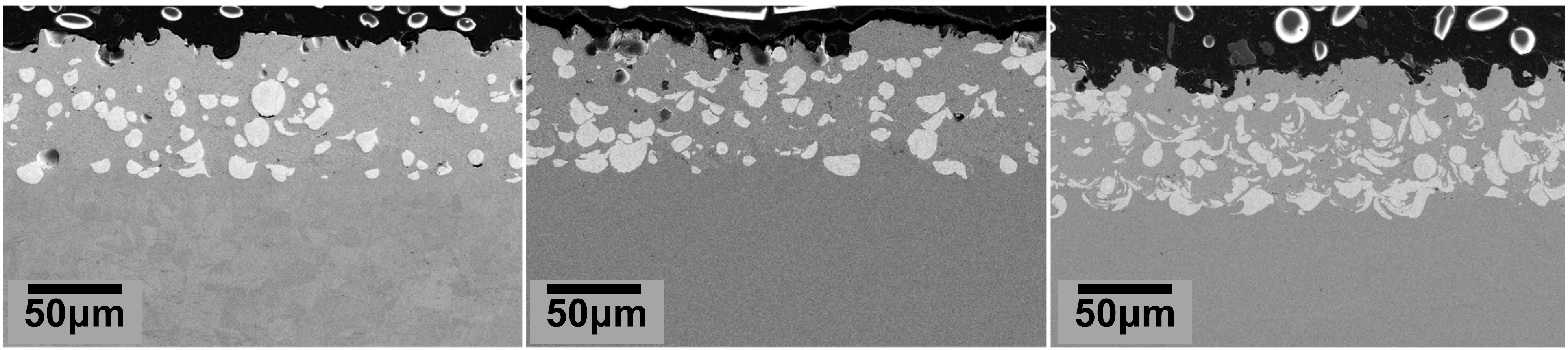

16 wt. % Ni | 10 wt. % Ni | 5 wt. % Ni

Coating thickness for all samples is ~ 75-90μm

16 wt.% Ni Coating – EDS Mapping

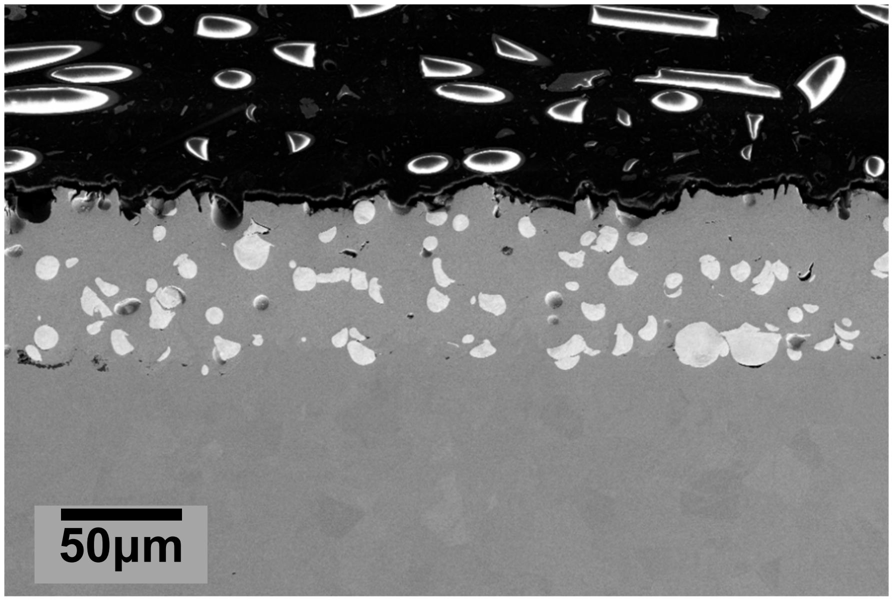

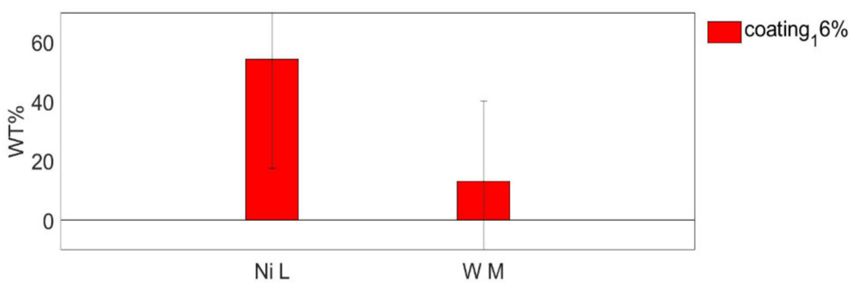

Area fraction of W – 14.7%

Measured using image analysis

Coating thickness ~75-90 μm

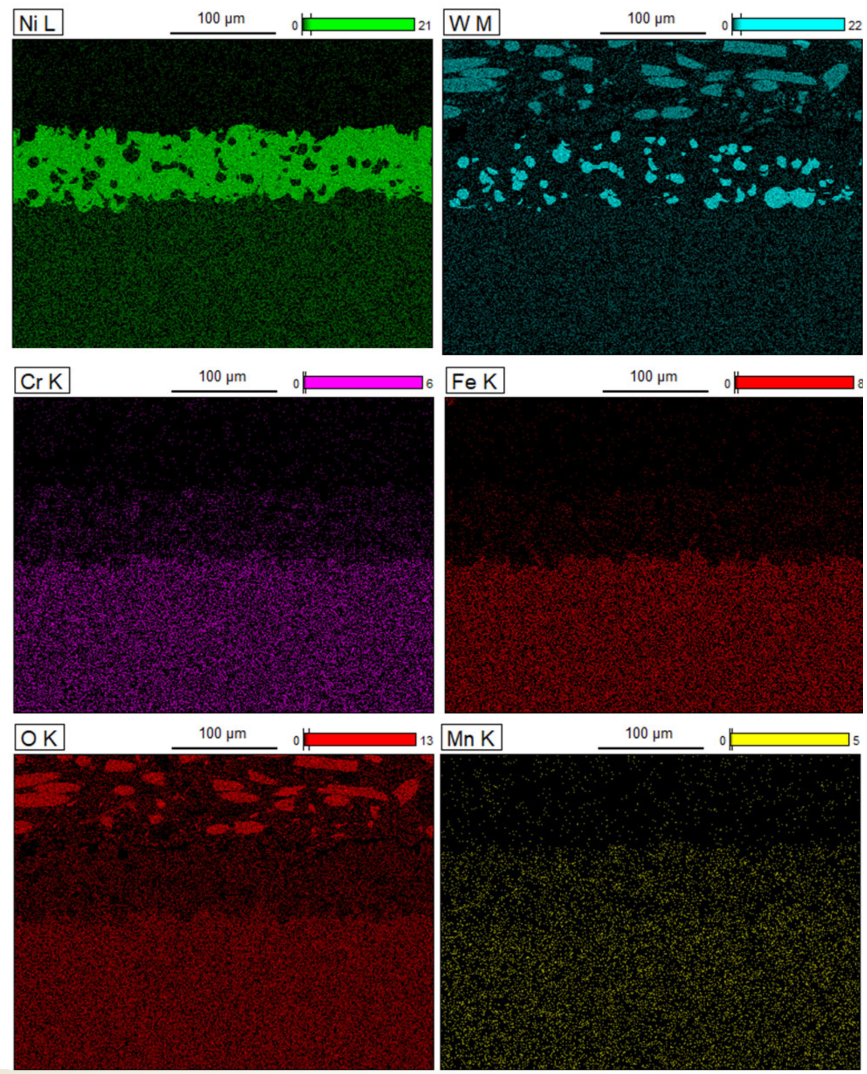

10 wt.% Ni Coating – EDS Mapping

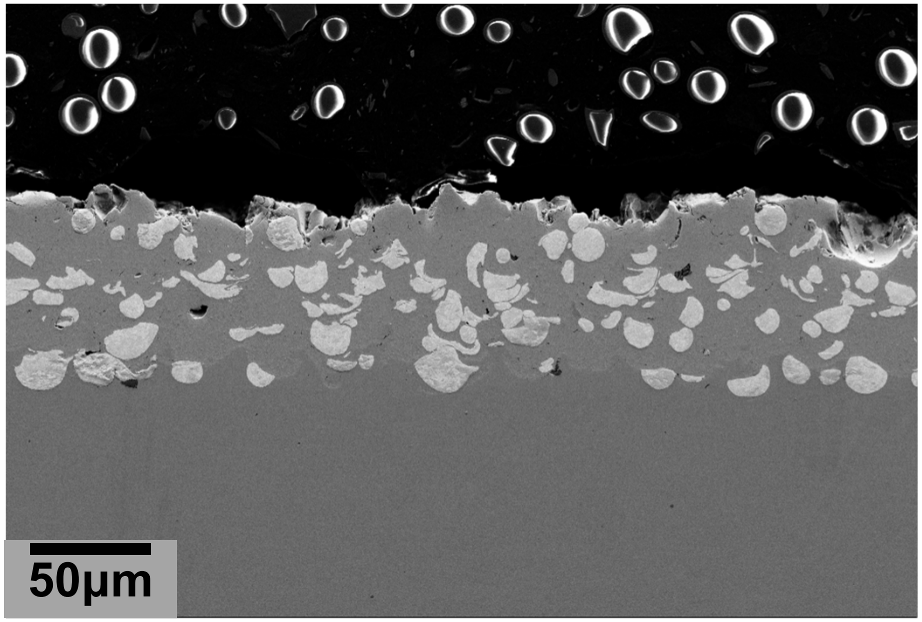

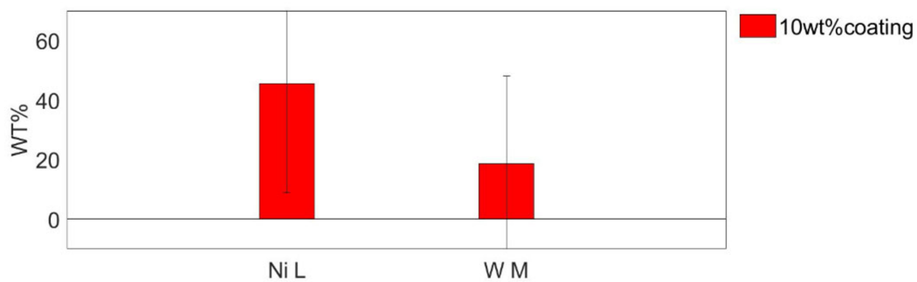

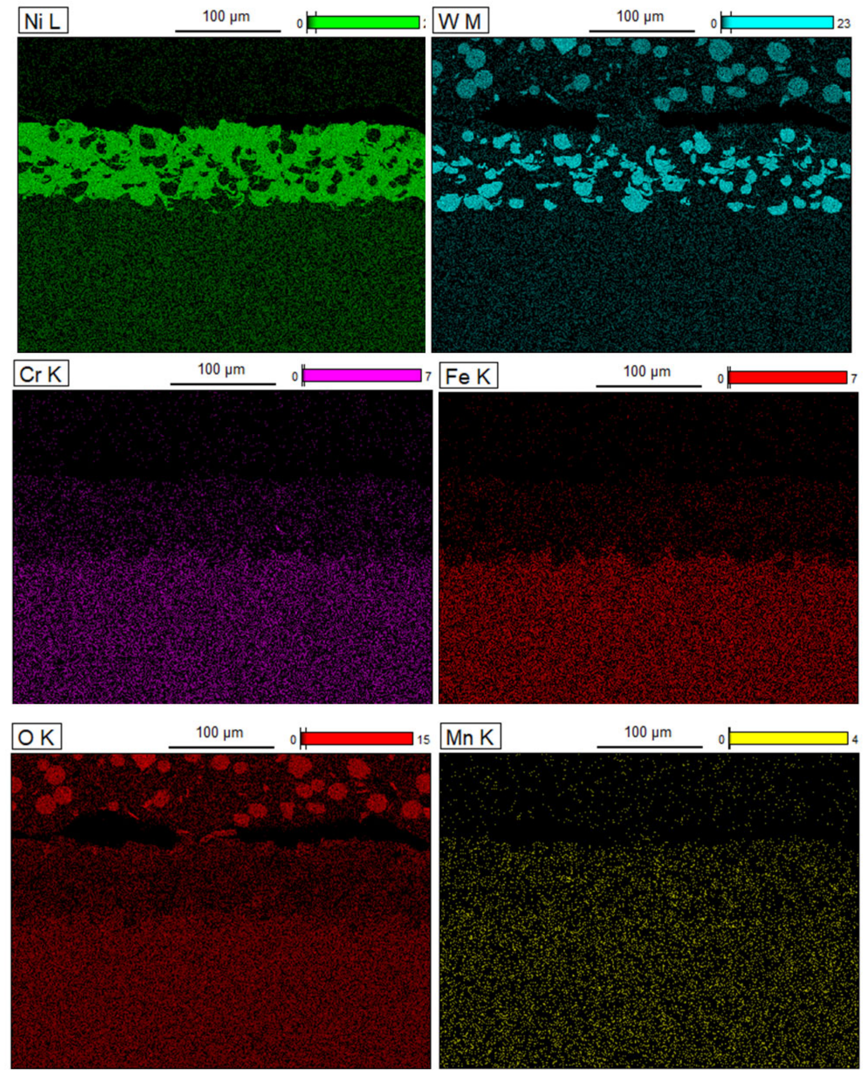

Area fraction of W – 22.6%

Measured using image analysis

Coating thickness ~75-90 µm

5 wt.% Ni Coating – EDS Mapping

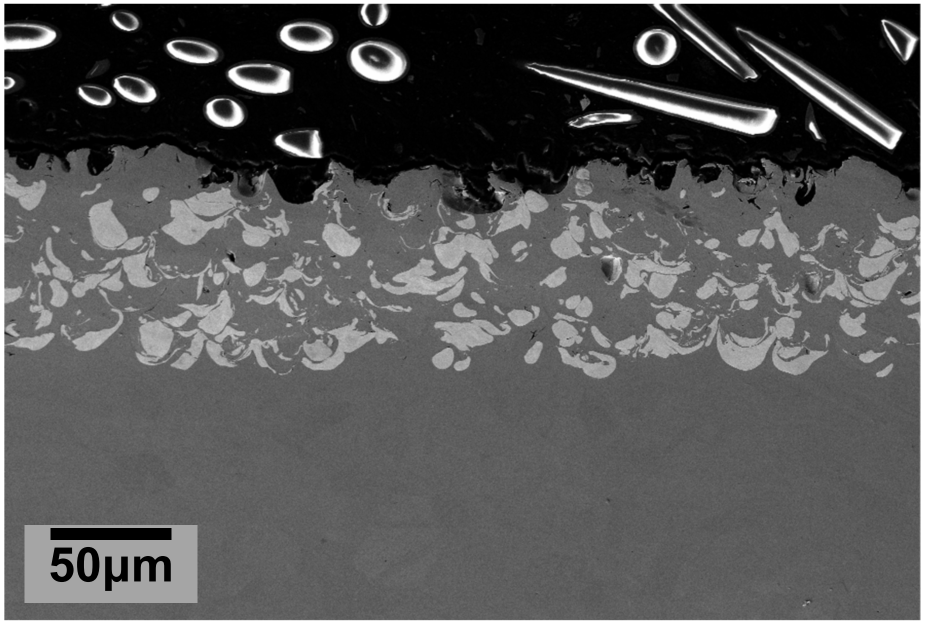

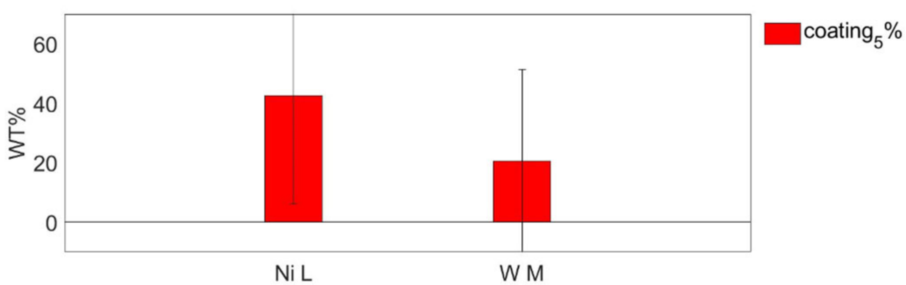

Area fraction of W – 27.3%

Measured using image analysis

Coating thickness ~75-90 µm

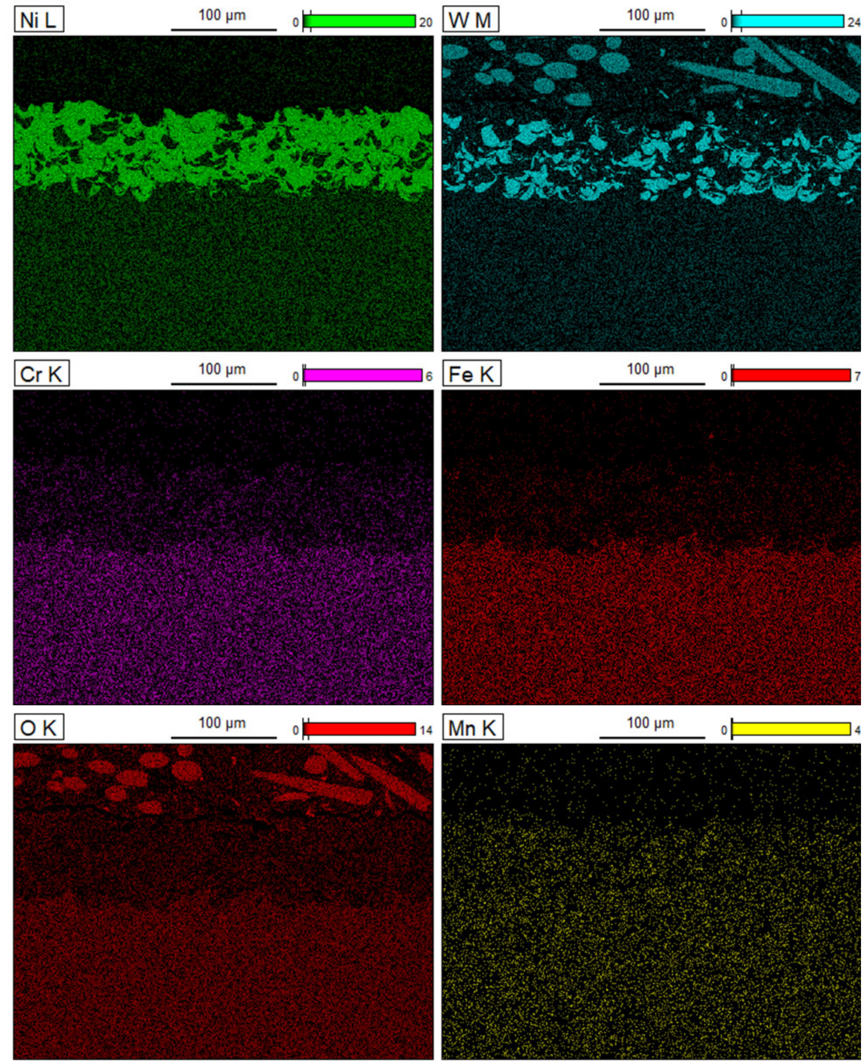

Coating from Ni-coated W powder particles

As-deposited Ni-coated W coating

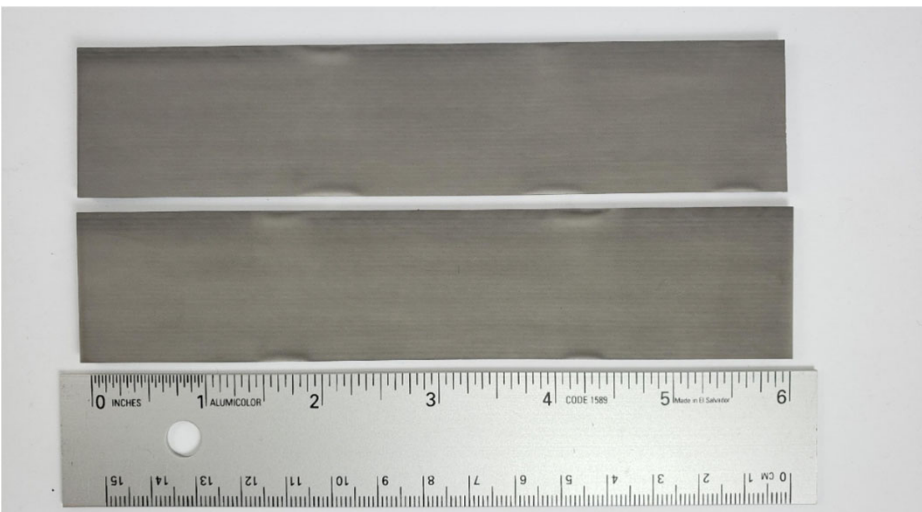

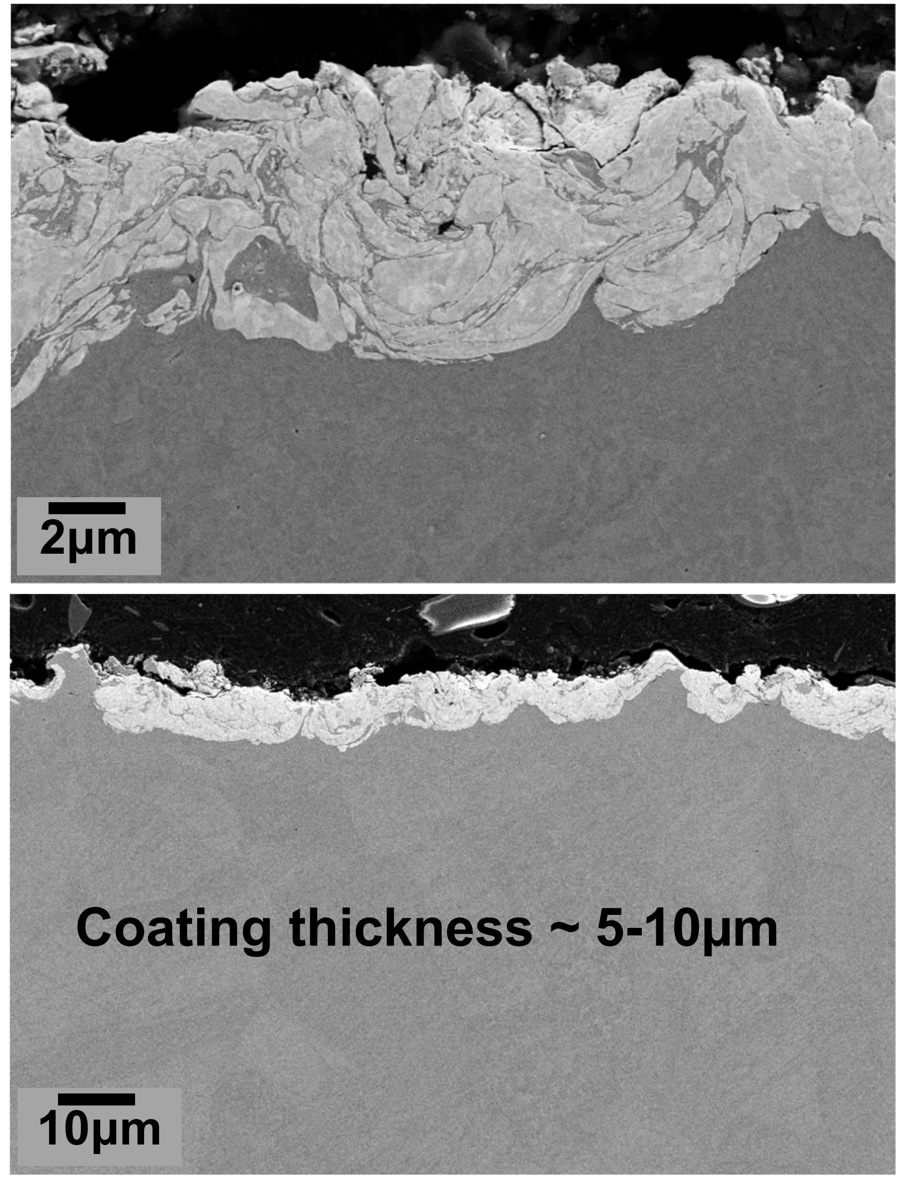

The Ni coating on the W powder particles was likely too thin to have any significant effect.

Thermal Cycle Test

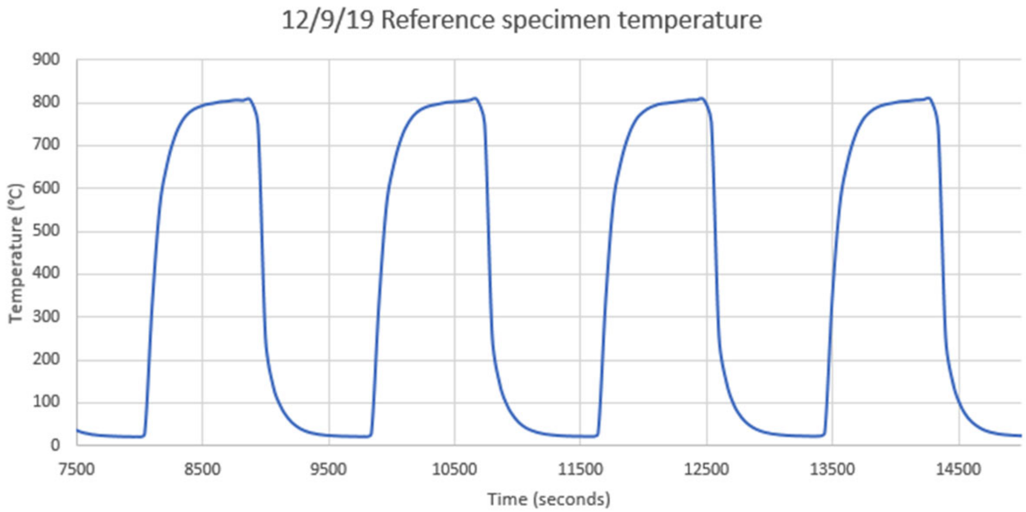

Blistered pure Ni coating after thermal cycling

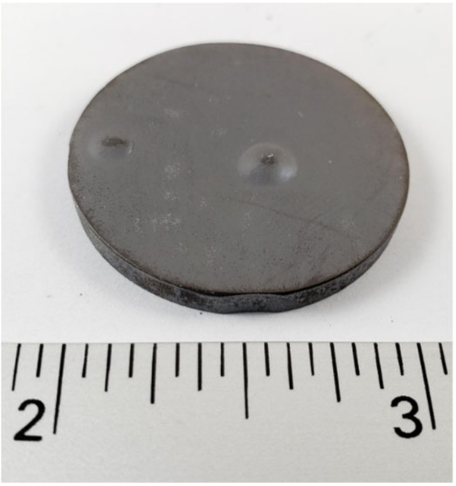

- Samples moved in and out of furnace between 25 °C and 800 °C
- Coatings well-adhered to the substrate
- Only pure Ni sample showed minor blistering (not Ni/W mixtures)

Work performed by Kairos Power

Interdiffusion Across Interface

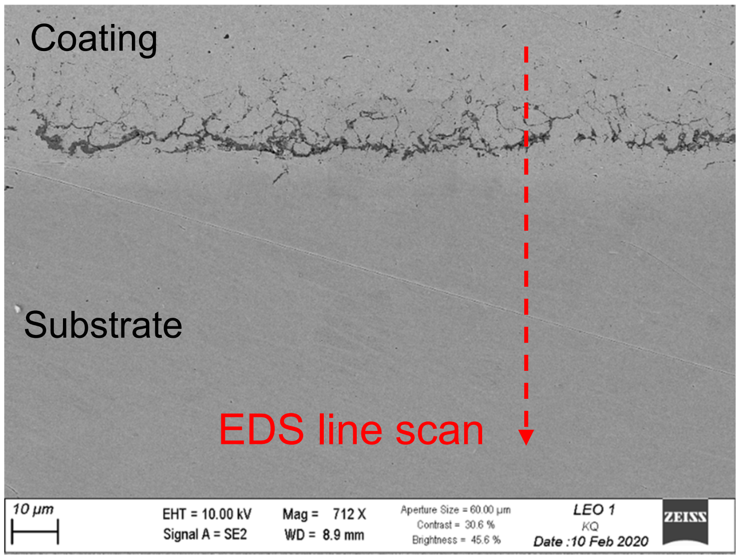

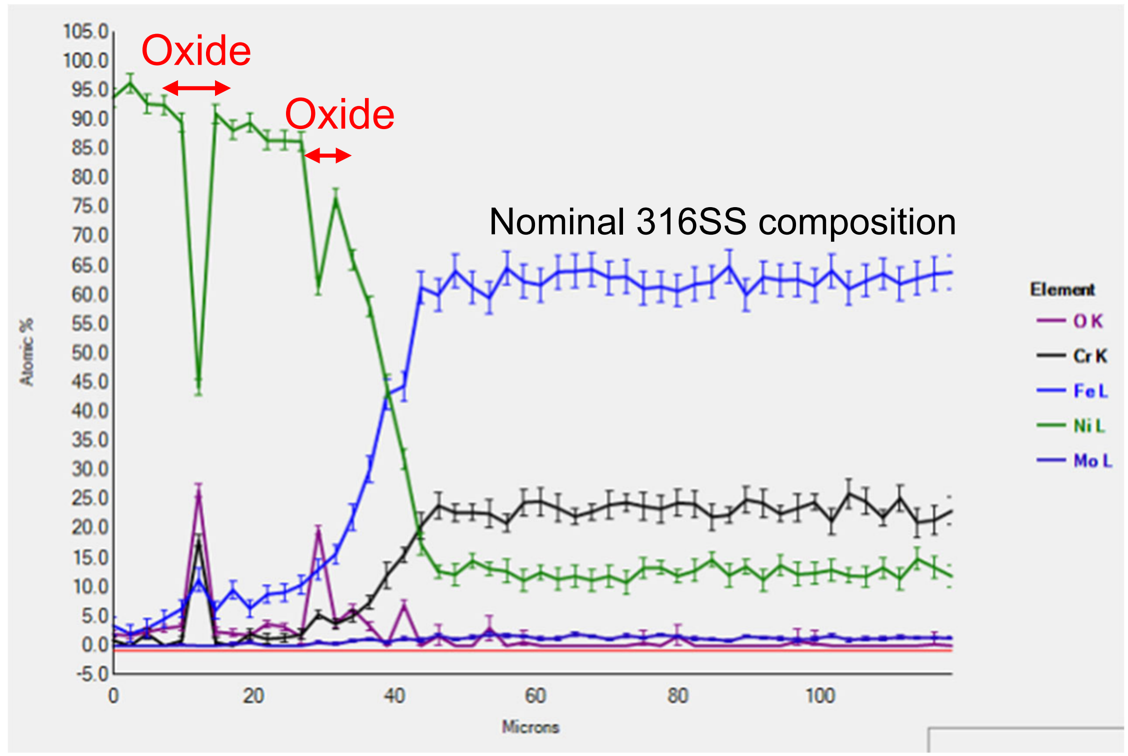

- Diffusion of Fe and Cr into Ni coating and diffusion of Ni into substrate is ~40µm deep

Deuterium Permeation Tests

The permeability was measured at 500°C, 600°C and 700°C to provide a baseline to determining permeation reduction factor (PRF)

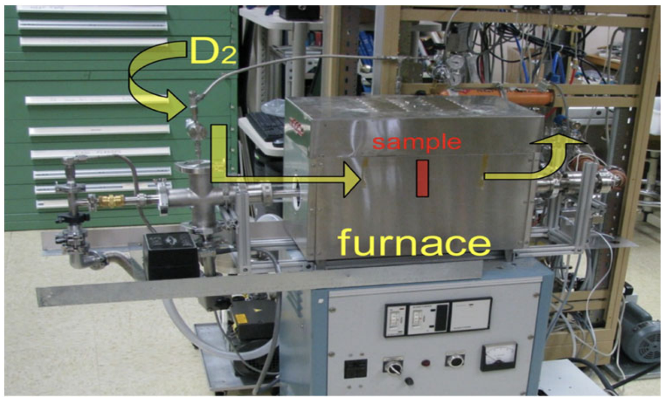

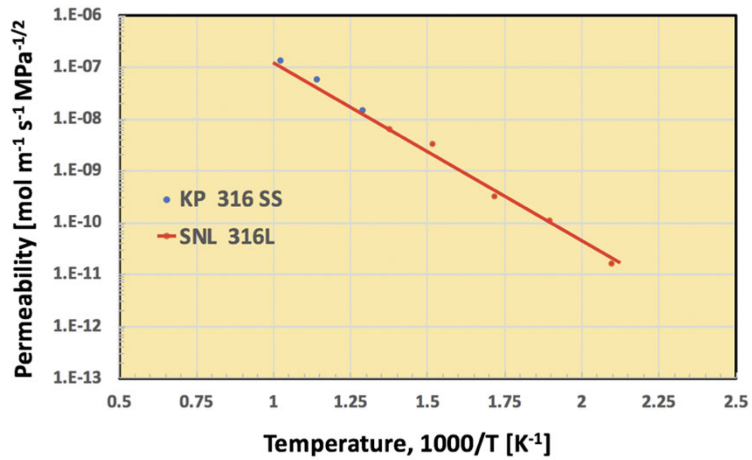

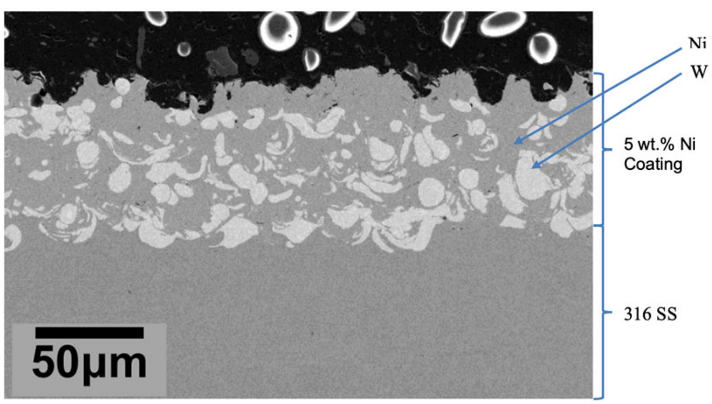

5 wt.% Ni Coating

No observable improvement in deuterium permeation resistance observed in these preliminary studies, but we intend to continue this work with other materials and compositions

Work performed by Kairos Power

Ti_2AlC Coatings Successfully Deposited: Example of a coating that <u>may</u> provide a combination of corrosion resistance and tritium diffusion resistance

As-deposited

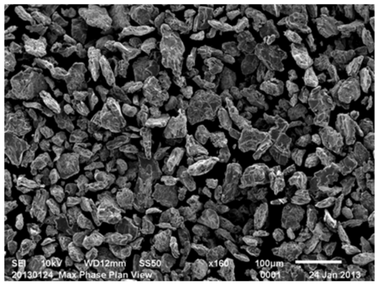

As-received powders

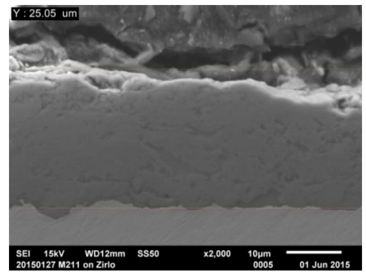

Cold sprayed coating

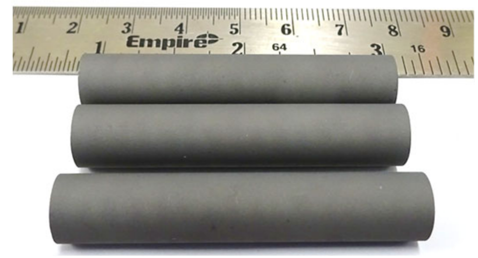

Coated cladding sections

After 1000°C test

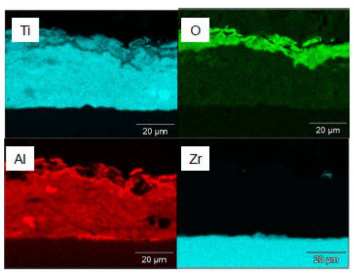

Underlying Zr-alloy protected

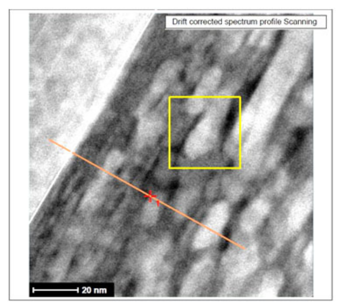

TEM of oxide layer alternating nanolaminates of Al_2O_3 and TiO_2

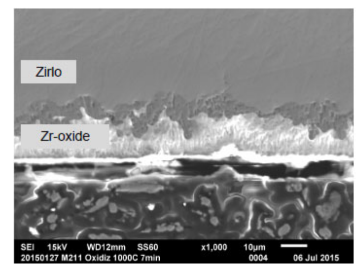

Severe oxidation on the uncoated Zirlo side

"Cold Spray Deposition of Ti_2AlC Coatings for Improved Nuclear Fuel Cladding", B.R. Maier, B.L. Garcia-Diaz, B. Hauch, L.C. Olson, R.L. Sindelar, and K. Sridharan, Journal of Nuclear Materials, 466, 2015, p. 712.

Contact Information and Questions

Kumar Sridharan

E-mail: kumar.sridharan@wisc.edu

Tel: 608-263-4789

University of Wisconsin
Cold Spray Laboratory